

PROGRESS REPORT

1995

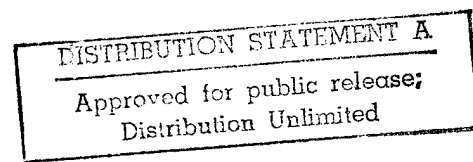
OF GRANT AFOSR F49620-92-J-0232-DEF (1992-1995)



by:

**Ernest Kun
Project Director**

*Approved for public release,
distribution unlimited*



REPORT DOCUMENTATION PAGE

1a. REPORT SECURITY CLASSIFICATION		1b. RESTRICTIVE MARKINGS			
2a. SECURITY CLASSIFICATION AUTHORITY		3. DISTRIBUTION/AVAILABILITY OF REPORT Approved for public release: Distribution unlimited.			
2b. DECLASSIFICATION/DOWNGRADING SCHEDULE					
4. PERFORMING ORGANIZATION REPORT NUMBER(S)		5. MONITORING ORGANIZATION REPORT NUMBER(S) AFOSR-JR-92-0380			
6a. NAME OF PERFORMING ORGANIZATION SFSU, Romberg Tiburon Ctr.	6b. OFFICE SYMBOL (If applicable)	7a. NAME OF MONITORING ORGANIZATION AFOSR/NL			
6c. ADDRESS (City, State, and ZIP Code) 3150 Paradise Drive Tiburon, CA 94920		7b. ADDRESS (City, State, and ZIP Code) 110 Duncan Ave Suite B115 Bolling AFB DC 20332-0001			
8a. NAME OF FUNDING/SPONSORING ORGANIZATION AFOSR	8b. OFFICE SYMBOL (If applicable) NL	9. PROCUREMENT INSTRUMENT IDENTIFICATION NUMBER F49620-92-J-0232			
10. SOURCE OF FUNDING NUMBERS					
		PROGRAM ELEMENT NO. 61102F	PROJECT NO. 2312	TASK NO. AS	WORK UNIT ACCESSION NO.
11. TITLE (Include Security Classification) Third and final technical report for F49620-92-0232-DEF					
12. PERSONAL AUTHOR(S) Dd. Ernest Kun, Principal Investigator and Project Director					
13a. TYPE OF REPORT Technical FINAL	13b. TIME COVERED FROM 4-1-94 TO 3-31-95	14 DATE OF REPORT (Year, Month, Day) 4-29-95	15. PAGE COUNT 137		
16. SUPPLEMENTARY NOTATION					
17. COSATI CODES		18. SUBJECT TERMS (Continue on reverse if necessary and identify by block number)			
FIELD	GROUP	SUB-GROUP			
19. ABSTRACT (Continue on reverse if necessary and identify by block number) Cellular proteins extracted from normal and cancer cells bind poly(ADP-ribose) polymerase on nitro-cellulose membrane blots. Histones at 1 mg/ml concentration completely prevent the binding of poly(ADP-ribose) polymerase to cellular proteins, indicating that the binding of histones to poly(ADP-ribose) polymerase sites competitively blocks the association of poly(ADP-ribose) polymerase to proteins other than histones. The direct binding of poly(ADP-ribose) polymerase to histones is shown by crosslinking with glutaraldehyde. The C-terminal basic histone H1 tail binds to the basic polypeptide domain of poly(ADP-ribose) polymerase. The basic domain present in the N-terminal part of core histones is the probable common structural feature of all core histones that accounts for their binding to poly(ADP-ribose) polymerase. Two polypeptide domains of poly(ADP-ribose) polymerase were identified, by way of CNBr fragments, to bind histones. These two domains are located within the 64 kDa fragment of poly(ADP-ribose) polymerase and are contiguous with the polypeptide domains that were shown to participate in self-association of poly(ADP-ribose) polymerase, ending at the 606th amino acid					
20. DISTRIBUTION/AVAILABILITY OF ABSTRACT <input type="checkbox"/> UNCLASSIFIED/UNLIMITED <input type="checkbox"/> SAME AS RPT <input type="checkbox"/> DTIC USERS			21. ABSTRACT SECURITY CLASSIFICATION		
22a. NAME OF RESPONSIBLE INDIVIDUAL Dr Walter Kozumbo			22b. TELEPHONE (Include Area Code) 202 - 767-5021	22c. OFFICE SYMBOL NL	

DD Form 1473, JUN 86

THIS FORM IS OBSOLETE

SERIAL NO. 851001 OF 1250

19950522 059

DTIC QUALITY ASSURANCE

05 MAY 1995

residue. The polypeptide domains of poly(ADP-ribose) polymerase which participate in DNA binding are thus shown to associate also with other proteins. Intact poly(ADP-ribose) polymerase binds to both the zinc-free or zinc-reconstituted basic polypeptide fragments of poly(ADP-ribose) polymerase. Histones activate auto-polymerase by increasing the number of short oligomers on poly(ADP-ribose) polymerase. This reaction is also dependent in a biphasic manner on the concentration of poly(ADP-ribose) polymerase. Histones in solution are only marginally poly-ADP-ribosylated but are good polymer acceptors when incorporated into artificial nucleosion structures.

Accesion For	
NTIS	CRA&I <input checked="" type="checkbox"/>
DTIC	TAB <input type="checkbox"/>
Unannounced <input type="checkbox"/>	
Justification	
By	
Distribution /	
Availability Codes	
Dist	Avail and / or Special
A-1	

Table of contents

I.	Table of contents	2
II.	Identification of domains of poly(ADP-ribose) polymerase for protein binding and self association	7
1.	Summary	8
2.	Introduction	10
3.	Materials and Methods	14
a.	Binding of poly(ADP-ribose) polymerase to cellular proteins	14
b.	Isolation of peptides of poly(ADP-ribose) polymerase obtained by proteases or CNBr	14
c.	Digestion of histone H1 with chymotrypsin	16
d.	Labeling of poly(ADP-ribose) polymerase or its fragments by ^{125}I	16
e.	Labeling of poly(ADP-ribose) polymerase by [32P]-ADP-ribose	17
f.	Labeling of DNA	17
g.	Electrophoretic techniques	17

h. Preparation of histone-Sepharose and poly(ADP-ribose) polymerase-Sepharose affinity matrices	18
i. Crosslinking of poly(ADP-ribose) polymerase with histone 2B with glutaraldehyde	18
j. Binding of labeled poly(ADP-ribose) polymerase and its polypeptides and labeled histones to transblotted peptides	19
k. Binding of labeled DNA to transblotted peptides	19
l. Incorporation of ^{65}Zn into transblotted zinc finger-containing peptides	20
m. Binding of the polypeptide fragments of poly(ADP-ribose) polymerase to histone-Sepharose and poly(ADP-ribose) polymerase-Sepharose affinity column	20
n. Poly(ADP-ribose) polymerase assay	21
o. Nucleosome reconstruction	21
p. Poly(ADP-ribose) chain length analysis	21
4. Results	22
a. The binding of ^{32}P -ADP-ribosylated poly(ADP-ribose) polymerase to histone H1 and its chymotryptic peptide fragments	28
b. The binding of [^{125}I]-labeled histone to chymotryptic fragments of poly(ADP-ribose) polymerase	32
c. Electrophoretic separation of CNBr fragments of poly-(ADP-ribose) polymerase eluted from a histone-Sepharose column	35

d.	The effect of histone H3 on the enzymatic activity of poly(ADP-ribose) polymerase	48
e.	The effect of histones on the chain length distribution of poly(ADP-ribose)	51
f.	Nucleosomal structure-dependent poly-ADP-ribosylation of histones	51
5.	Discussion	57
6.	References	61
III.	Reversion of malignant phenotype by 5-iodo-6-amino-1,2-benzopyrone, a noncovalently binding ligand of poly(ADP-ribose) polymerase	68
1.	Summary	69
2.	Introduction	70
3.	Materials and Methods	71
4.	Results and Discussion	72
5.	References	82
IV.	Phosphorylation of poly(ADP-ribose) polymerase protein in human peripheral lymphocytes stimulated with phytohemagglutinin	83
1.	Summary	84
2.	Introduction	85
3.	Materials and Methods	87
a.	Human blood lymphocytes	87
b.	Peripheral blood	87

c.	Cell count & blast cell count & cell cycle stages	87
d.	Permeabilization of cells.....	88
e.	Immunoprecipitation	89
f.	Intracellular protein kinase C activity	89
g.	Poly(ADP-ribose) polymerase and Protein kinase C purification	90
4.	Results	91
5.	Discussion	105
6.	References	108
V.	Specific disulfide formation in the oxidation of HIV-1 zinc finger protein nucleocapsid p7	111
1.	Summary	112
2.	Introduction	113
3.	Experimental Section	115
a.	Chemicals	115
b.	Protein preparation	115
c.	Oxidation of reconstituted p7	116
d.	Oxidation of denatured apo p7	116
e.	Mass spectrometric analysis	116
f.	Properties of oxidized p7 and apo p7	117

4.	Results	119
a.	Reaction of NOBA and Cu ²⁺ with Zn-reconstituted p7	119
b.	Reaction of Noba With apo p7	124
c.	Identification of the positions of disulfide bonds	124
5.	Discussion	129
6.	References	134

**IDENTIFICATION OF DOMAINS OF POLY(ADP-RIBOSE) POLYMERASE FOR PROTEIN
BINDING AND SELF-ASSOCIATION**

Summary

Cellular proteins extracted from normal and cancer cells bind poly(ADP-ribose) polymerase on nitro-cellulose membrane transblots. Histones at 1 mg/ml concentration completely prevent the binding of poly(ADP-ribose) polymerase to cellular proteins, indicating that the binding of histones to poly(ADP-ribose) polymerase sites competitively blocks the association of poly(ADP-ribose) polymerase to proteins other than histones. The direct binding of poly(ADP-ribose) polymerase to histones is shown by crosslinking with glutaraldehyde. The C-terminal basic histone H1 tail binds to the basic polypeptide domain of poly(ADP-ribose) polymerase. The basic domain present in the N-terminal part of core histones is the probable common structural feature of all core histones that accounts for their binding to poly(ADP-ribose) polymerase. Two polypeptide domains of poly(ADP-ribose) polymerase were identified, by way of CNBr fragments, to bind histones. These two domains are located within the 64 kDa fragment of poly(ADP-ribose) polymerase and are contiguous with the polypeptide domains that were shown to participate in self-association of poly(ADP-ribose) polymerase, ending at the 606th amino acid residue. The polypeptide domains of poly(ADP-ribose) polymerase which participate in DNA binding are thus shown to associate also with other proteins. Intact poly(ADP-ribose) polymerase binds to both the zinc-free or zinc-reconstituted basic polypeptide fragments of poly(ADP-ribose) polymerase. Histones activate auto-poly-ADP-ribosylation of poly(ADP-ribose) polymerase by increasing the number of short

oligomers on poly(ADP-ribose) polymerase. This reaction is also dependent in a biphasic manner on the concentration of poly(ADP-ribose) polymerase. Histones in solution are only marginally poly-ADP-ribosylated but are good polymer acceptors when incorporated into artificial nucleosome structures.

Introduction

Poly(ADP-ribose) polymerase (ADP-ribose transferase, polymerizing, E.C.2.4.2.30) is a highly abundant nuclear protein of higher eukaryotes (1,2) that exhibits at least two catalytic functions: ADP-RIBOSE polymerizing and NAD glycohydrolase activities, which are also regulated by the state of differentiation of particular cell types (3).

Assuming the same molecular activity *in vitro* and *in vivo*, poly(ADP-ribose) polymerase activity in maximally stimulated cells appears to account for only one percent of the molecular activity of this enzyme (1,2), approximating the magnitude detectable in the isolated homogeneous protein in the absence of coenzymic DNA (4), an activity present even in the 56 kDa polypeptide fragment of poly(ADP-ribose) polymerase (5) that contains no DNA recognition sites (6). These observations suggest that the enzymatic activity of poly(ADP-ribose) polymerase is highly regulated in physiologically operating cells.

Immunochemical estimation of native and automodified poly(ADP-ribose) polymerase in intact cells in culture (AA-2 and MT-2 cells) indicated that only 4% (for AA-2) or 20% (for MT-2) of poly(ADP-ribose) polymerase was auto-ADP-ribosylated, thus a significant portion of this protein is available for macromolecular associations (7). Indeed recent results (8) show that *in vitro* poly(ADP-ribose) polymerase significantly stimulates DNA polymerase α but not β . Microinjection of the 46 kDa DNA-binding polypeptide fragment of poly(ADP-ribose) polymerase into human fibroblasts inhibits MNNG-induced unscheduled DNA synthesis

(56), further supporting the contention that protein-protein or protein-DNA interactions involving poly(ADP-ribose) polymerase may have biological consequences. Binding of poly(ADP-ribose) polymerase to the DNA primer of HIV reverse transcriptase was also shown to inhibit this enzyme (9). A potentially important cellular function of poly(ADP-ribose) polymerase in NAD⁺-dependent repair of damaged DNA *in vitro* has been also traced to the release of the binding of poly(ADP-ribose) polymerase from DNA termini by auto-poly-ADP-ribosylation of the enzyme protein (10,11). Self-association (dimerization) of poly(ADP-ribose) polymerase has been shown to be essential for auto-poly-ADP-ribosylation of the enzyme protein (12,13). Furthermore, binding to and trans-ADP-ribosylation (14) to an assortment of highly significant enzymes that act on DNA, such as the calcium/magnesium-dependent endonuclease (15), DNA polymerase α and β , terminal deoxynucleotidyl transferase, DNA ligase II (16,17), topoisomerase I (18,19), and topoisomerase II (20) are also of critical cell biochemical significance, because trans-ADP-ribosylation to these enzymes produces a down-regulation of their catalytic activities. As we show here, the binding of poly(ADP-ribose) polymerase on a large number of proteins, extracted from 3T3, CHO and PC12 cells, occurs readily in protein transblots on nitrocellulose membranes (Fig. 1), emphasizing the significant protein-protein associative capacity of poly(ADP-ribose) polymerase. We also show that histones by apparent competition can completely inhibit the binding of poly(ADP-ribose) polymerase to cellular proteins, suggesting that poly(ADP-ribose) polymerase-histone association and the association

of poly(ADP-ribose) polymerase with other cellular proteins may occur at the same poly(ADP-ribose) polymerase site. It follows that a more detailed analysis of poly(ADP-ribose) polymerase-histone association may shed light on the general poly(ADP-ribose) polymerase-protein binding sites of poly(ADP-ribose) polymerase. Clarification of poly(ADP-ribose) polymerase-protein binding in terms of identification of binding domains on poly(ADP-ribose) polymerase may have cell biological importance since inhibitors of poly(ADP-ribose) polymerase which do not inhibit poly(ADP-ribose) catabolism eventually convert cellular poly(ADP-ribose) polymerase to a protein- and DNA-binding cellular component that can regulate complex cellular processes (5,7,10,11,21). As a beginning to this highly involved series of poly(ADP-ribose) polymerase-protein interactions we first determined histone and self- association sites of poly(ADP-ribose) polymerase by nitrocellulose transblot binding and protein crosslinking methods. The study of binding kinetics of proteins in solution is subject to further experimental work.

In and of itself, poly(ADP-ribose) polymerase-histone binding is a significant biochemical problem. By far the most abundant nuclear proteins that are trans-ADP-ribosylated by poly(ADP-ribose) polymerase are histones (22) and we have demonstrated the *in vivo* occurrence of poly-ADP-ribosylated histones by specific antibodies directed against the polymer (23). Besides serving as ADP-RIBOSE acceptors (24) under certain conditions histones also activate rates of poly-ADP-ribosylation

(25). In stimulated thymocytes histone H3 is selectively poly-ADP-ribosylated (26). Apart from the binding of the zinc fingers of poly(ADP-ribose) polymerase to DNA termini (27), molecular details of protein-protein associations of poly(ADP-ribose) polymerase are unknown. We report here the identification of binding domains on poly(ADP-ribose) polymerase for histones which probably represent general protein binding sites including a self-association site of the poly(ADP-ribose) polymerase enzyme protein , and provide evidence for a regulatory effect of these sites on enzymatic activity.

Materials and Methods

Electrophoretically 98% homogeneous poly(ADP-ribose) polymerase and coenzymic DNA were isolated from calf thymus as reported (28, 29). Unavoidable traces of lower-mass bands were peptides of poly(ADP-ribose) polymerase produced by proteases as identified by immunotransblots (28). The isolated protein did not contain covalently bound poly-ADP-ribose as determined by the absence of binding to phenylboronate affinity columns (7). The commercial sources of reagents were as follows: CNBr-activated Sepharose 4B and the Mono S column from Pharmacia (Piscataway, NJ), Affi-Gel 10 from Bio-Rad (Richmond, CA), [³²P]-NAD⁺ and the [¹²⁵I]-Bolton-Hunter reagent from ICN (Irvine, CA), [⁶⁵Zn]-ZnCl₂ from Du Pont-NEN (Wilmington, DE) and Centricon concentrators from Amicon (Danvers, MA). Histones were obtained from Sigma Chemical Co. All other chemicals used were of the highest purity available.

Binding of poly(ADP-ribose) polymerase to cellular proteins. 3T3, CHO and PC12 cells were grown and harvested by scraping into Dulbecco's phosphate buffered saline without Ca²⁺ and Mg²⁺ at midconfluent state. Cells were washed twice with Dulbecco's phosphate buffered saline without Ca²⁺ and Mg²⁺ to remove medium and finally were resuspended into Dulbecco's phosphate buffered saline without Ca²⁺ and Mg²⁺. Aliquots of 2x10⁵ cells were withdrawn and mixed with electrophoretic sample buffer, boiled for five minutes and then

loaded onto 10% SDS-PAGE gels made according to Laemmli (30). After electrophoresis, proteins were transblotted onto nitrocellulose membranes, renatured and the aspecific binding sites on the membrane were blocked with bovine albumin. Membrane bound proteins were probed with [¹²⁵I]-poly(ADP-ribose) polymerase (10 µg, 4x10⁵ cpm) either in the absence or in the presence of 1mg/ml histone H1 for 30 minutes at 23°C.

Isolation of polypeptides of poly(ADP-ribose) polymerase obtained by proteases or CNBr cleavage. Partial digestion of poly(ADP-ribose) polymerase with chymotrypsin (31) was done as follows. poly(ADP-ribose) polymerase (2 mg/ml in 50 mM Tris-HCl, 200 mM NaCl, 20 mM 2-mercaptoethanol, pH 8.0) was digested with 3.3 µg/ml chymotrypsin at 25°C for 30 minutes, then the reaction was stopped with 1 mM phenylmethylsulfonyl fluoride and the polypeptides isolated by ion exchange chromatography on the Mono S column as reported (6). The basic N-terminal 64 kDa polypeptide eluted at 0.45 M NaCl from the cation exchanger column. The C-terminal 56 kDa polypeptide, which did not bind to the cation exchanger, was isolated on a benzamide-Affigel 10 affinity column as described earlier (6).

Cyanogen bromide (CNBr) fragments of poly(ADP-ribose) polymerase were prepared by the following technique. Homogeneous poly(ADP-ribose) polymerase (200 µg) was precipitated with 20% TCA, and pelleted by centrifugation, washed with 70% ethanol and dried. The dried

protein was dissolved in 100 μ l of 88% formic acid, and 300 μ l of 0.1 M HCl and 20 μ l of CNBr (100 mg/ml in ethanol) were added and the mixture allowed to stand for 48 hours at room temperature. Then the solvent was evaporated by freeze-drying and the residue dissolved in 400 μ l of "renaturation buffer"(32).

Digestion of poly(ADP-ribose) polymerase with plasmin was carried out as described earlier (6).

Digestion of histone H1 with chymotrypsin (33, 34). Histone H1 (70 μ g) was digested with 0.12 μ g of chymotrypsin for 25 minutes at 25°C in 45 μ l 0.1 M Tris-HCl (pH 8.0). The reaction was stopped by addition of phenylmethylsulfonyl fluoride (1 mM final concentration).

Labeling of poly(ADP-ribose) polymerase or its fragments by ^{125}I . The polypeptides to be labeled with ^{125}I were dissolved in 25-50 μ l of 150 mM phosphate (pH 8.2) and pipetted into Eppendorf centrifuge tubes, which contained 2 μ l of [^{123}I]-Bolton-Hunter reagent (1888 Ci/mmol, 33 μ Ci in benzene-dimethylformamide) previously evaporated to dryness by a stream of N₂. After mixing by aspiration into the tip of a micropipette several times, the iodination reaction was allowed to proceed at 6°C for 1 hour. The unreacted Bolton-Hunter reagent was quenched with 5 μ l of 1 M Tris-HCl (pH 9.0) and the reaction mixture gel-filtered through an 1.5 ml Sephadex G25 (fine) column equilibrated with 0.1 M sodium phosphate buffer (pH 7.5) containing 0.1% gelatin. The exclusion volume contained the iodinated polypeptides. The

incorporation of ^{125}I was in the range of 3 to 5%. The ^{125}I -labeled protein was used on the same day of its preparation for binding experiments.

Labeling of poly(ADP-ribose) polymerase by $[^{32}\text{P}]\text{-ADP-RIBOSE}$.

This was carried out by incubating the protein with 25 nM of $[^{32}\text{P}]\text{-NAD}^+$ as described earlier (14).

Labeling of DNA. Sonicated calf thymus DNA, average length 250 bp, was used for labeling. The DNA (50 μg) was dissolved in 100 μl of Klenow buffer containing 50 μM dNTPs and 10 mCi of $[^{32}\text{P}]\text{-TTP}$ and then enzymatically end-labeled with Klenow fragment of DNA Pol I as described (35). The labeled DNA was purified by phenol extraction and ethanol precipitation.

Electrophoretic techniques. poly(ADP-ribose) polymerase and its chymotryptic fragments were separated by 10% SDS-PAGE (30), and histones or CNBr fragments of poly(ADP-ribose) polymerase by a 17.5% acrylamide-SDS system as described (36). Electroblotting was carried out in 10 mM 3-[cyclohexylamino]-1-propanesulfonic acid (CAPS)-NaOH (pH 11.0) buffer containing 15% methanol for 90 minutes using nitrocellulose membranes with 0.45 mm pore size. When amino acid sequencing was performed, PVDF membranes (ProBlot membrane, Applied Biosystems, Foster City, CA) were used and the excised pieces containing the transblots of peptides were sequenced using the Model

470-A gas-phase sequencer and an on-line 120A PHT-analyzer (Applied Biosystems, Foster City, CA) according to a published method (37).

Preparation of histone-Sepharose and poly(ADP-ribose) polymerase-Sepharose affinity matrices. Affinity matrices were prepared from CNBr-activated Sepharose 4B and histones or purified bovine poly(ADP-ribose) polymerase, according to the manufacturer's protocol. The amount of proteins bound to the matrix was determined in 0.1 ml aliquots of the settled resin by a published method (38). On the average 0.9-1.2 mg of histones and 2 mg of poly(ADP-ribose) polymerase were covalently bound per 1 ml packed bed of the gel matrix.

Crosslinking of poly(ADP-ribose) polymerase with Histone2B with glutaraldehyde (12). Histone 2B was labelled with ^{125}I using the Bolton-Hunter reagent. The unbound labeling was removed by gel filtration. poly(ADP-ribose) polymerase (3.2 ug) and [^{125}I]-Histone 2B (3 μg ; 5×10^4 cpm) were incubated either alone or in combination with 8mM of glutaraldehyde in a 40 μl volume reaction mixture containing 50 mM triethanolamine-HCl buffer (pH 8.0) for 10 minutes at 23°C . After incubation 10 μl of 5x sample buffer (made according to Laemmli) was added and loaded onto 5-20% SDS-PAGE gradient gels without prior boiling. In addition, 1/50th of each sample was loaded onto another gel for immunological characterization. After electrophoresis part of the samples were stained with Coomassie blue , destained, dried and autoradiographed while the other gel was developed as a western blot .

Binding of labeled poly(ADP-ribose) polymerase and its polypeptides and labeled histones to transblotted peptides. Membranes containing electroblotted peptides were soaked in "renaturation buffer", 50 mM Tris-HCl (pH 8.0), 100 mM NaCl, 1 mM DTT and 0.3% Tween 20 (32) for 1 hour then blocked by incubation with 2% defatted powdered milk (dissolved in Dulbecco's phosphate buffered saline without Ca²⁺ and Mg²⁺ containing 0.1 mM phenylmethylsulfonyl fluoride) for 2-6 hours at 25°C (37). The membranes were then washed with a "low salt buffer" (50 mM Tris-HCl (pH 7.5), 10 mM 2-mercaptoethanol, 0.1 mM phenylmethylsulfonyl fluoride, 0.05% BSA and 0.05% Tween 20). The incubation with labeled polypeptides ($2-5 \times 10^5$ cpm, 2-5 mg) was performed in the same buffer (15-25 ml) as the one used for washing for 30 minutes at 25°C. Then the membranes were washed once with the low salt buffer and twice with the low salt buffer containing 50 mM NaCl. Finally they were dried and exposed overnight to X-ray film. Polypeptides of histone H1 obtained by chymotrypsin and pepsin digestion were isolated as reported (33,34,39).

Binding of labeled DNA to transblotted peptides. Polypeptides transblotted to membranes were renatured (32) and blocked with defatted milk, then washed once with 0.1 M potassium phosphate buffer, (pH 7.6) containing 1 mM EDTA, and incubated in the same buffer (15 ml) with [³²P]-DNA ($5-10 \times 10^4$ cpm, 2-4 mg) for 20 min. at 25°C. After four

washings with the same buffer the membranes were dried and exposed to X ray films overnight.

Incorporation of $[^{65}\text{Zn}]$ into transblotted zinc finger-containing peptides. Transblotted peptides were renatured (32) in the presence of 5 mCi $[^{65}\text{Zn}]\text{-ZnCl}_2$ in 10 ml renaturation buffer for one hour at 25°C, then the membranes washed with renaturation buffer until no radioactivity over background was found in the washings. The membranes were exposed to X-ray films to locate $[^{65}\text{Zn}]$ -containing bands.

Binding of the polypeptide fragments of poly(ADP-ribose) polymerase to histones-Sepharose and poly(ADP-ribose) polymerase-Sepharose affinity column. A histones-Sepharose column (1 ml bed volume) was loaded with 50 mg of CNBr fragments dissolved in 0.4 ml of 50 mM Tris-HCl, (pH 8.0) containing 10 mM 2-mercaptoethanol and allowed to bind for 30 minutes at 25°C. The column was then stepwise eluted with 2 ml aliquots of the above buffer containing increments of NaCl: 50, 100, 200, 400 and 1000 mM. The eluted fractions were concentrated on Centricon 3, and one-third of the total amount of concentrates applied onto 17.5% SDS-PAGE. After separation, the gel was stained with Coomassie blue, or transblotted onto PVDF membranes for sequencing.

poly(ADP-ribose) polymerase-Sepharose columns (1 ml bed volume) were loaded with either 50 µg of histone H1 or its chymotryptic

polypeptides. Chromatography was carried out exactly as described above.

Poly(ADP-ribose) polymerase assay. The assays were carried out by published techniques (6) with modifications as given in the figure legends.

Nucleosome Reconstruction (40). Coenzymic DNA (600 mg) and an equal amount of core histones were dissolved in 1.5 ml of 10 mM Tris-HCl, 1 mM EDTA, pH 8.0 (10 mM Tris-HCl, 0.2 mM EDTA, pH 7.4) containing 0.8 M NaCl. This solution was dialyzed (at 4°C) stepwise against 10 mM Tris-HCl, 1 mM EDTA, pH 8.0 that contained progressively lower concentrations of NaCl (0.8, 0.6, 0.4 and 0.2 M NaCl). Each dialysis step lasted 90 minutes, except the final dialysis against 10 mM Tris-HCl, 1 mM EDTA, pH 8.0 containing no added NaCl was extended overnight. The DNA content was adjusted to 200 mg/ml by dilution.

Poly(ADP-ribose) chain length analysis was carried out according to Althaus et al (41) using DNA sequencing type gels.

Results

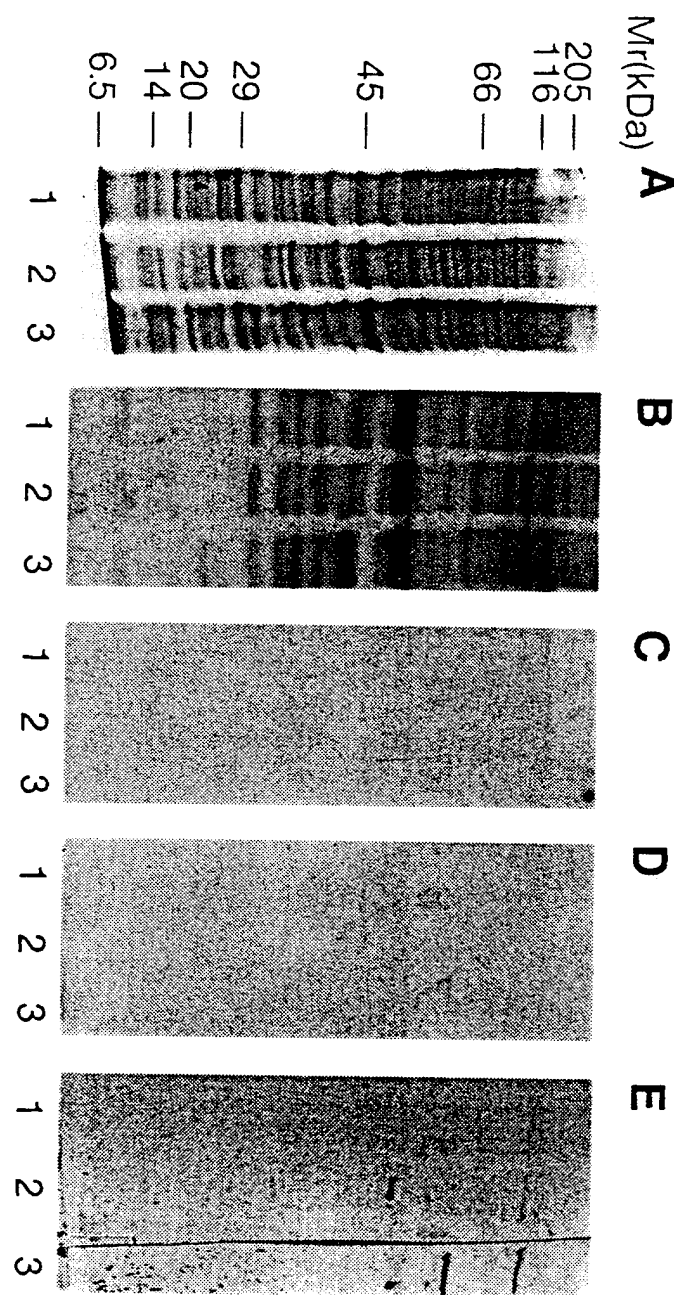
The binding of poly(ADP-ribose) polymerase to cellular proteins extracted from three cell types is shown in Fig. 1. Among the numerous protein fractions separated by gel electrophoresis (Fig. 1, Panel A) upon transblot to nitrocellulose membranes approximately 16-20 major bands adsorbed [¹²⁵I]-labeled poly(ADP-ribose) polymerase to varying extents. (Fig. 1, Panel B). When the binding experiment was repeated in the presence of 1 mg/ml of histone H1 added to the binding mixture, poly(ADP-ribose) polymerase exhibited no association with the transblotted cellular proteins (Fig. 1, Panel C). Histone H1 could be replaced by any other histone (not shown). A similar inhibition of binding occurred in the presence of 0.5 M NaCl, a salt concentration usually required to extract poly(ADP-ribose) polymerase from nuclei (28). It was also found that the assay for poly(ADP-ribose) polymerase binding to other polypeptides or the binding of poly(ADP-ribose) polymerase-derived peptides to histones was limited by the size of the polypeptide, which was 6-10 kDa, and no association by this technique could be detected if the polypeptide was of a smaller size. This size limitation puts some constraints on binding experiments employing the transblot technique, as will be shown below. When the presence of poly(ADP-ribose) polymerase in extracts of 2×10^5 cells was probed with poly(ADP-ribose) polymerase-specific polyclonal antibody (28), faint bands were seen in 3TC and CHO cells (Fig. 1, Panel E, Lanes 1,2) and

Figure 1. The binding of poly(ADP-ribose) polymerase to cellular proteins, their inhibition by histone H1 and 0.5 M NaCl.

Panel A. Electrophoretically separated cellular proteins on transblots were stained with Ponceau S (see Methods). Lane 1, 3T3 cells; Lane 2, CHO cells; Lane 3, PC12 cells.

Panel B. Autoradiography identifying the binding of [¹²⁵I]-poly(ADP-ribose) polymerase (10 µg, 4 x 10⁵ cpm) to the cellular proteins on transblots, as described in Panel A. Lane 1, 3T3 cells; Lane 2, CHO cells; Lane 3, PC12 cells. Panel C. The binding experiment, as shown in Panel B, was performed in the presence of 1 mg/ml solution of histone H1. Panel D. The binding assay shown in panel B was performed in the presence of 0.5 M NaCl. Panel E. Immunochemical assay for poly(ADP-ribose) polymerase antibody-reactive proteins shown in Panel A. The same amounts of cellular proteins were employed in experiments shown in panels A-E, hence the faint immunopositive poly(ADP-ribose) polymerase bands shown in Panel E, Lanes 1 and 2, indicate apparently smaller concentrations of poly(ADP-ribose) polymerase in 3T3 and CHO cells.

Fig. 1



stronger bands, including a proteolytic degradation product of poly(ADP-ribose) polymerase, were detectable in the extract of the more malignant PC12 cells (Fig.1, Panel E, Lane 3).

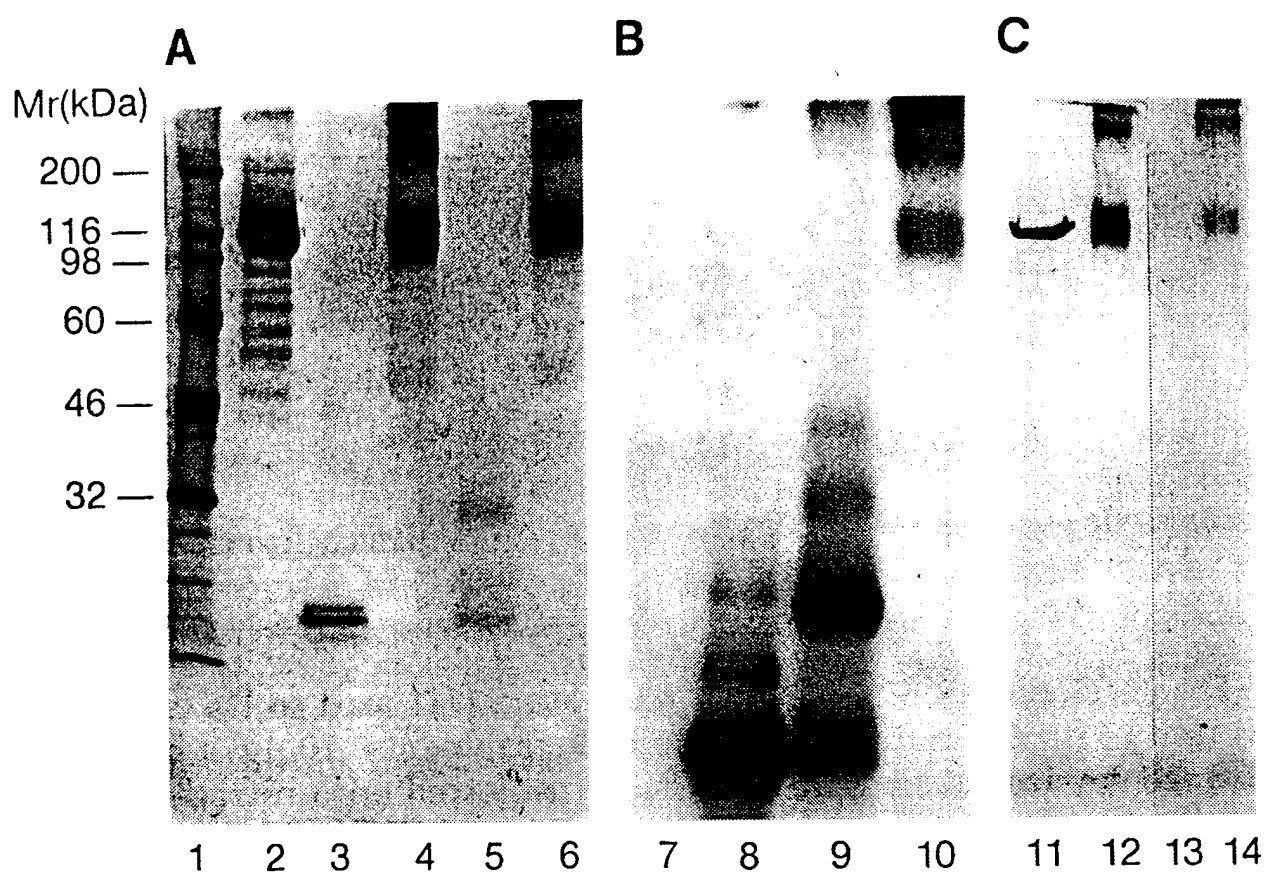
Since histones prohibited the association of poly(ADP-ribose) polymerase with other cellular proteins, implying that histones effectively competed at protein binding sites of poly(ADP-ribose) polymerase with other proteins, we reasoned that determination of histone-binding polypeptide domains of poly(ADP-ribose) polymerase may identify general protein association sites. The prerequisite for this assumption was a direct demonstration of the association of histones with poly(ADP-ribose) polymerase, which was carried out by the glutaraldehyde crosslinking technique (12) as shown in Fig.2. In Panel A of Fig. 2, Coomassie blue-stained protein bands identify poly(ADP-ribose) polymerase and histone 2B separately but not in the crosslinked complex (Lanes 4 & 6) because of the limited resolving power of SDS-PAGE. In the autoradiography shown in Panel B of Fig. 2, unlabeled poly(ADP-ribose) polymerase (Lane 7) gave no signal, whereas [¹²⁵I]-labeled histone 2B (Lane 8) and glutaraldehyde crosslinked histone 2B (Lane 9) clearly separated from the poly(ADP-ribose) polymerase-[¹²⁵I]-labeled-histone 2B crosslinked product, which is shown in Lane 10. The poly(ADP-ribose) polymerase component of the crosslinked poly(ADP-ribose) polymerase-histone 2B complex was identified by immunoblot (Fig. 2, Panel C). Lane 11 is poly(ADP-ribose) polymerase, Lane 12 is glutaraldehyde crosslinked poly(ADP-ribose)

Figure 2. Crosslinking with glutaraldehyde of histone 2B with poly(ADP-ribose) polymerase.

Panel A. Coomassie blue-stained proteins. Lane 1, molecular weight standards; Lane 2, poly(ADP-ribose) polymerase and degradation products; Lane 3, [^{125}I]-labeled histone 2B; Lane 4, glutaraldehyde-crosslinked poly(ADP-ribose) polymerase; Lane 5, glutaraldehyde-crosslinked [^{125}I]-labeled histone H2B; Lane 6, glutaraldehyde-crosslinked [^{125}I]-labeled histone H2B with poly(ADP-ribose) polymerase.

Panel B. Autoradiography of labeled proteins given in Panel A. Lane 7, unlabeled poly(ADP-ribose) polymerase; Lane 8, [^{125}I]-labeled histone H2B; Lane 9, same as Lane 8 except crosslinked with glutaraldehyde; Lane 10, glutaraldehyde crosslinked poly(ADP-ribose) polymerase with [^{125}I]-labeled histone H2B. Panel C. Identification of poly(ADP-ribose) polymerase component in Panel B by immunoblot. Lane 11, poly(ADP-ribose) polymerase; Lane 12, crosslinked poly(ADP-ribose) polymerase; Lane 13, histone H2B; Lane 14, crosslinked poly(ADP-ribose) polymerase with [^{125}I]-labeled histone H2B.

Fig. 2



polymerase and Lane 14 is the adduct of poly(ADP-ribose) polymerase with glutaraldehyde crosslinked [^{125}I]-labeled-histone 2B, containing also some glutaraldehyde crosslinked dimers of poly(ADP-ribose) polymerase. Lane 13 contains histone H2B which does not react with anti-poly(ADP-ribose) polymerase serum.

The binding of ^{32}P -ADP-ribosylated poly(ADP-ribose) polymerase to histone H1 and to its chymotryptic peptide fragments. Proteolytic fragments of histone H1 (33, 34, 39) fulfilled physical requirements for binding assays, and as shown in Fig. 3, the C-terminal basic histone tail of H1 readily binds to poly(ADP-ribose) polymerase, implying that this lysine-rich polypeptide domain is the probable common denominator that provides binding of all types of histones to poly(ADP-ribose) polymerase. The poly(ADP-ribose) polymerase binding lysine-rich histone domain is in the carboxy terminal of histone H1, but in core histones this polypeptide is part of the amino terminal (42, 43). Figure 3A illustrates the electrophoretic separation of histone H1 (Lane 1) and its chymotryptic fragments (Lane 2) stained by Ponceau red, whereas the binding of labeled poly(ADP-ribose) polymerase to histone H1 is shown in Lane 3, and to chymotryptic fragments of histone H1 in Lane 4. The binding of histone H1 and its chymotryptic C-terminal polypeptide to the poly(ADP-ribose) polymerase affinity column is demonstrated in Fig. 3B which is a Coomasie blue-stained gel (for details see legend of Fig. 3B). Since histone H1 (Fig. 3B, Lane 12) and its C-terminal tail (Lane 5) both elute with 200 mM NaCl, their affinity to the poly(ADP-ribose) polymerase

Figure 3. Binding of poly(ADP-ribose) polymerase to histone H1 and to its chymotryptic fragments.

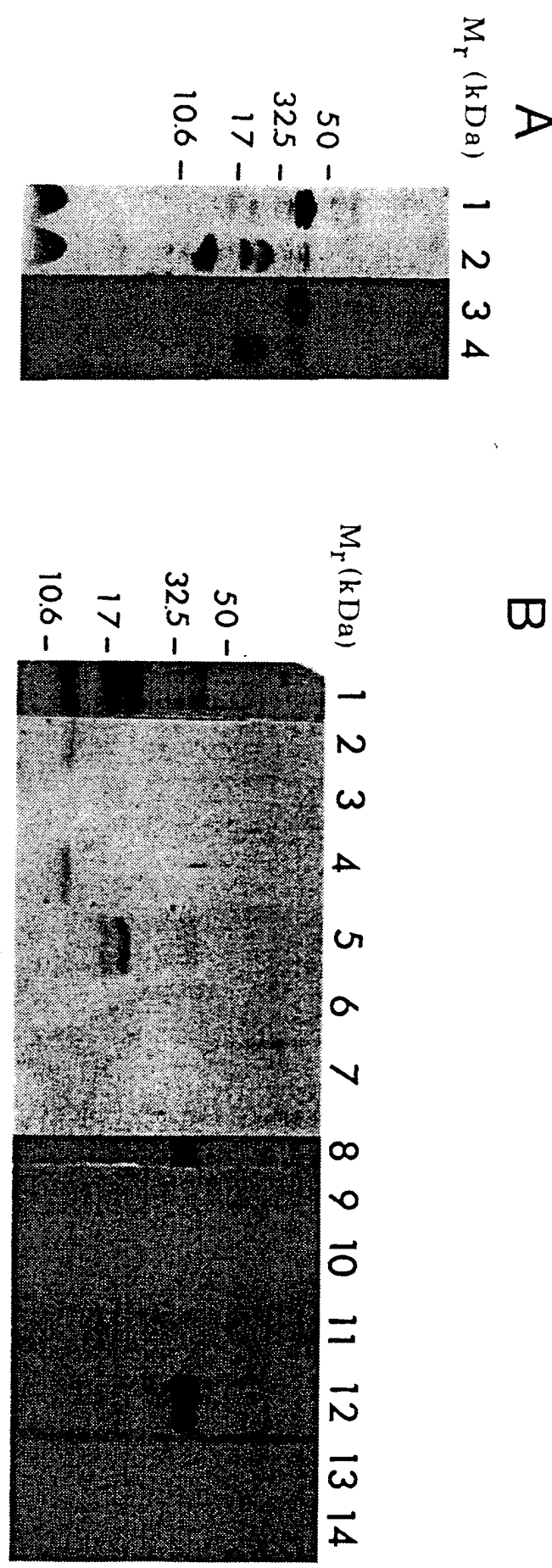
Fig. 3A. The binding of [^{32}P]-ADP-ribosylated poly(ADP-ribose) polymerase to histone H1 and to its chymotryptic polypeptide fragments. 10 μg of histone H1 (Lanes 1 and 3) and 10 μg of chymotrypsin-digested histone H1 (Lanes 2 and 4) were separated by SDS-PAGE, transblotted onto nitrocellulose membranes and probed with ^{32}P -ADP-ribosylated poly(ADP-ribose) polymerase (3 μg , 10⁵ cpm; obtained by incubating poly(ADP-ribose) polymerase with 25 nM [^{32}P]-NAD⁺ for 10 minutes followed by gel filtration on a Sephadex G75 column) and then processed (see Materials and Methods). Lanes 1 and 2 are Ponceau Red-stained polypeptides and Lanes 3 and 4 are autoradiograms. The doublets in lanes 2 and 4 (17, 18 kDa) are the C-terminal basic fragments of histone H1.

Fig. 3B. The binding of histone H1 and its chymotryptic fragments to poly(ADP-ribose) polymerase-Sepharose affinity columns. The poly(ADP-ribose) polymerase-Sepharose columns were loaded either with chymotryptic fragments of 50 μg of histone H1 (Lanes 1-7) or with

(Figure 3, continued)

50 µg of histone H1 (Lanes 8-14). The columns were then eluted with NaCl solutions with increasing ionic strength and aliquots from each fraction were loaded onto SDS-PAGE gels, electrophoresed and Coomassie blue-stained. Lane 1 shows polypeptides of histone H1 obtained by chymotryptic digestion; Lanes 2 and 9 are flow-through fractions with buffer only; Lanes 3 and 10 are eluates with 50 mM NaCl; Lanes 4 and 11 are eluates with 100 mM NaCl; Lanes 5 and 12 are eluates with 200 mM NaCl. Lanes 6 and 13 are eluates with 400 mM NaCl and Lanes 7 and 14 are eluates with 1000 mM NaCl, indicating that there are no further absorbed polypeptides present in the adsorbed form.

Fig. 3

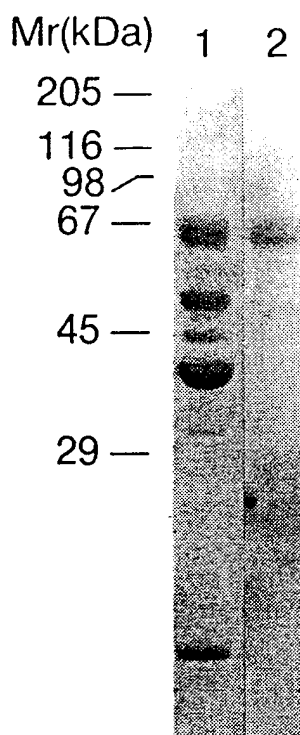


column appears to be identical. A weak binding of the N-terminal fragment is also apparent (Fig. 3B, Lane 4). However this weak association does not show up in the nitrocellulose binding assay (Fig. 3A, Lanes 3 and 4) that is carried out under more stringent conditions, therefore the main poly(ADP-ribose) polymerase-binding C-terminal tail of histone H1 is the significant poly(ADP-ribose) polymerase- binding histone polypeptide. The N-terminal CNBr fragment of histone H4 - as predicted - binds to poly(ADP-ribose) polymerase in the same manner as the C-terminal chymotryptic fragment of H1 (not shown). According to published results (41) the poly(ADP-ribose) polymerase-binding histone fragments bind also free poly(ADP-ribose).

The binding of [¹²⁵I]-labeled histones to chymotryptic fragments of poly(ADP-ribose) polymerase. The binding of polypeptides derived from poly(ADP-ribose) polymerase by chymotryptic digestion to a mixture of radioiodinated core histones was assayed on nitrocellulose membranes. The separation of chymotryptic polypeptides of poly(ADP-ribose) polymerase, mainly representing molecular masses of 64 kDa, 56 kDa and 42 kDa are shown (Coomassie-blue stained) in Lane 1 of Fig. 4, coinciding with published results (31). When the chymotryptic polypeptides of poly(ADP-ribose) polymerase were transblotted onto nitrocellulose membranes and incubated with radioiodinated core histones, only the basic polypeptide of poly(ADP-ribose) polymerase (64 kDa) indicated histone binding (Fig. 4, Lane 2).

Figure 4. Binding of labeled histones to transblotted chymotryptic fragments of poly(ADP-ribose) polymerase. The digestion of poly(ADP-ribose) polymerase, separation of polypeptides, electroblotting onto a nitrocellulose membrane and the procedure for binding [¹²⁵I]-histones are described in Materials and Methods. Lane 1: Coomassie blue-stained peptides, Lane 2: autoradiography of bound [¹²⁵I]-histones to transblotted peptides of poly(ADP-ribose) polymerase.

Fig. 4

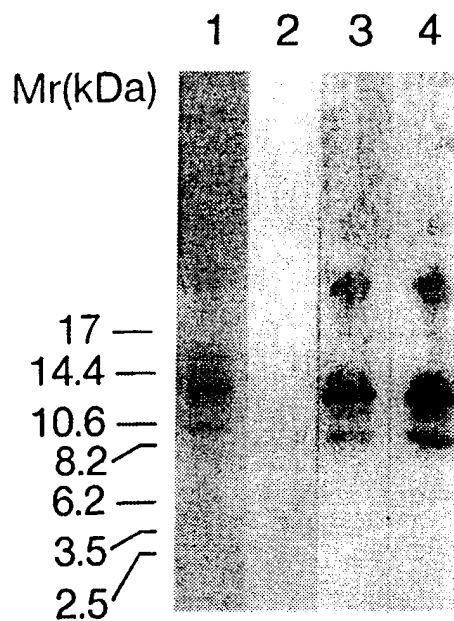


The correctness of these conclusions was tested also by "opposite" labeling, i.e. radioiodination of polypeptides of poly(ADP-ribose) polymerase. The same results as shown in Fig. 4 were obtained, i.e. only the basic half of poly(ADP-ribose) polymerase bound to histones, regardless which protein species was labeled with ^{125}I . Fig. 5, Lane 1 shows the Coomassie blue-stained histones (mixed histones; 8 $\mu\text{g}/\text{Lane}$). Lane 2 illustrates that the 56 kDa polypeptide (labeled with ^{125}I) of poly(ADP-ribose) polymerase (the catalytic domain) did not bind to transblotted histones at all. The binding of the labeled basic 64 kDa polypeptide to transblotted histones is apparent from Lane 3 together with Lane 4, a positive control where the binding of labeled intact poly(ADP-ribose) polymerase protein to histones is shown. The intact protein bound to transblotted histones in the same manner as the 64 kDa basic polypeptide (compare Lanes 3 and 4).

Electrophoretic separation of CNBr fragments of poly(ADP-ribose) polymerase eluted from a histone-Sepharose column. A more detailed localization of histone binding sites on poly(ADP-ribose) polymerase was achieved by percolating CNBr-generated peptide fragments of poly(ADP-ribose) polymerase through a histone-Sepharose affinity matrix and identifying the bound fragments. From the known amino acid sequence of bovine poly(ADP-ribose) polymerase (44) it is predictable that CNBr fragments of poly(ADP-ribose) polymerase in the region between zinc finger II and the catalytic domain yield peptides of 8-18 kDa size, which

Figure 5. Binding of [^{125}I]-labeled poly(ADP-ribose) polymerase and its N-terminal and C-terminal fragments to transblotted histones. Four mg of mixed histones were electrophoresed (36) then transblotted onto nitrocellulose membranes and probed with ^{125}I -labeled poly(ADP-ribose) polymerase. Lane 1 shows Coomassie blue-stained histones, all the other lanes are autoradiograms. The absence of binding of radiolabeled 56 kDa polypeptide of poly(ADP-ribose) polymerase to histones is shown in Lane 2. Lanes 3 and 4 illustrate the histone binding of the labeled 64 kDa polypeptide and of the entire poly(ADP-ribose) polymerase protein as a control.

Fig. 5



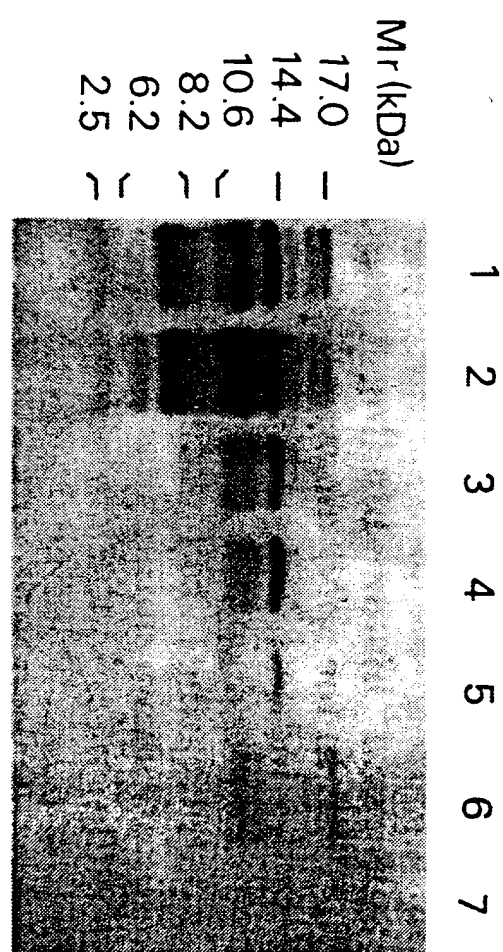
are large enough to bind to poly(ADP-ribose) polymerase. In contrast, CNBr fragmentation of the zinc finger region produces some very short peptides which would not bind to poly(ADP-ribose) polymerase because of their small size. Adsorption of CNBr fragments to the histone matrix, followed by elution with a salt solution of stepwise increasing ionic strength permits an estimation of the relative binding strength of polypeptides to the histone matrix. Electrophoretic separation of CNBr fragments of poly(ADP-ribose) polymerase is shown in Fig. 6, Lane 1. In Lane 2, the non-adsorbed (flow-through) fragments, eluted by 50 mM Tris-HCl (pH 8.0) containing 10 mM 2-mercaptoethanol, are demonstrated. Lanes 3 to 7 show fragments emerging at 50 (Lane 3), 100 (Lane 4), 200 (Lane 5), 400 (Lane 6) and 1000 mM NaCl (Lane 7) as components of the elution buffer. The polypeptide with an apparent mass of 14 kDa eluted between 50 and 200 mM NaCl, accompanied (Lanes 3 and 4) by a broader immunopositive band which most probably consists of proteolytic breakdown products of this fragment.

The 14 kDa polypeptide was identified by sequencing and corresponds to residues 186-290 on the sequence of poly(ADP-ribose) polymerase (105 residues, $M_r = 11,826$), its N-terminal being GFSVL.... . This polypeptide is located between the 29 and 36 kDa domains of poly(ADP-ribose) polymerase obtained by digestion with plasmin (6). It is only 22 residues downstream of the second zinc finger as apparent from the domain diagram (Fig. 7). We also sequenced the fragments which elute at 0.4 M

Fig 6. Electrophoretic separation of CNBr fragments of poly(ADP-ribose) polymerase eluted from a histone-Sepharose affinity column.

Lane 1 shows CNBr- generated peptides prior to passing through the affinity matrix; Lane 2, the flow-through CNBr fragments; Lanes 3-7, the eluates with 50, 100, 200, 400, 1000 mM NaCl respectively. For technical details, see Materials and Methods.

Fig. 6



NaCl (apparent M_r 10 kDa and 18 kDa, shown in Fig. 6, Lane 6). The N-terminus of the 18 kDa peptide was XXLTLGXLSQ... . This sequence places the peptide on the bovine enzyme at 396-525 (130 residues, $M_r = 14,002$). Sequencing of the 10 kDa fragment yielded an N-terminal sequence of XEVKEANIRV... . The position of this peptide is at 446-525 (80 residues, $M_r = 8,603$). These two poly-peptides thus partly overlap, the larger includes the smaller one which is adjacent to the 56 kDa catalytic domain. These two poly peptides are part of the automodifiable region (45) of poly(ADP-ribose) polymerase and only the shorter one is shown as histone binder in Fig. 7.

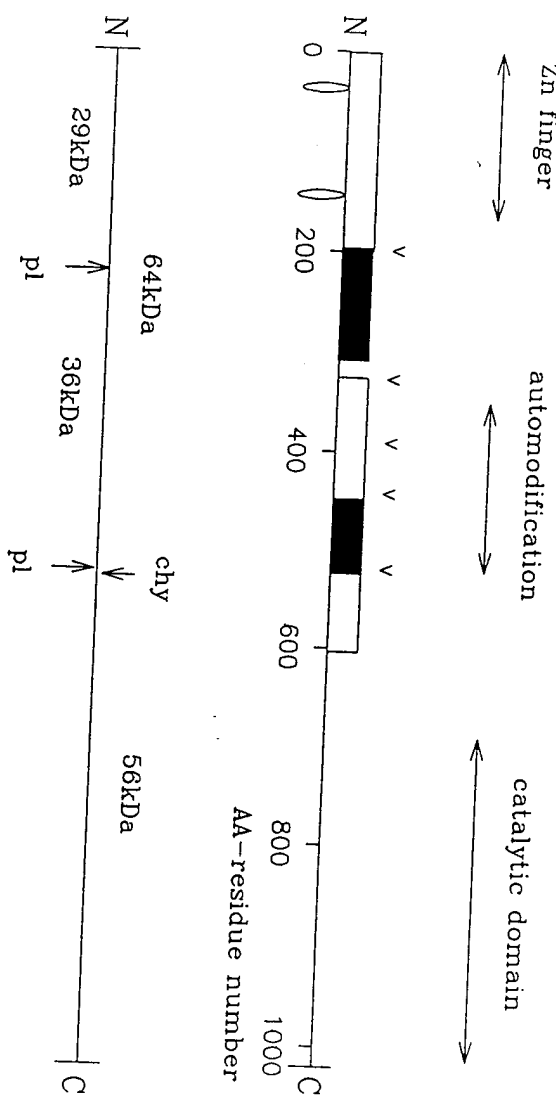
Our results are consistent with the existence of two histone-binding regions, one between residues 186 and 290, which is close to the second zinc finger, and a second histone- binding sequence that is between residues 446 and 525 that is part of the automodifiable portion of poly(ADP-ribose) polymerase (Fig. 7).

Since both direct chemical (12) and kinetic (13) evidence supports the significance of self-association of poly(ADP-ribose) polymerase molecules, we attempted to identify polypeptide domains of poly(ADP-ribose) polymerase that are participatory in the self-binding reaction. Chemical crosslinking experiments (12) earlier identified the 36 and 29 kDa polypeptides as binding to each other, implying self-association. When the poly(ADP-ribose) polymerase protein was digested with plasmin (6) a degradation pattern of polypeptides occurs as visualized

Fig. 7. Self- and histone-binding sites of poly(ADP-ribose) polymerase. In the upper diagram shaded rectangles indicate histone-binding CNBr peptides and open rectangles are peptides participating in self-binding. The lower diagram shows cutting sites by proteases. Small ellipses in the upper diagram mark the position of zinc-fingers. N: the N-terminal, C: the C-terminal, pl: plasmin cutting sites, chy: chymotryptic cutting sites. The sign v identifies the N-termini of polypeptides obtained by direct sequencing. Established polypeptide domains of poly(ADP-ribose) polymerase are also indicated with double ended arrows.

43

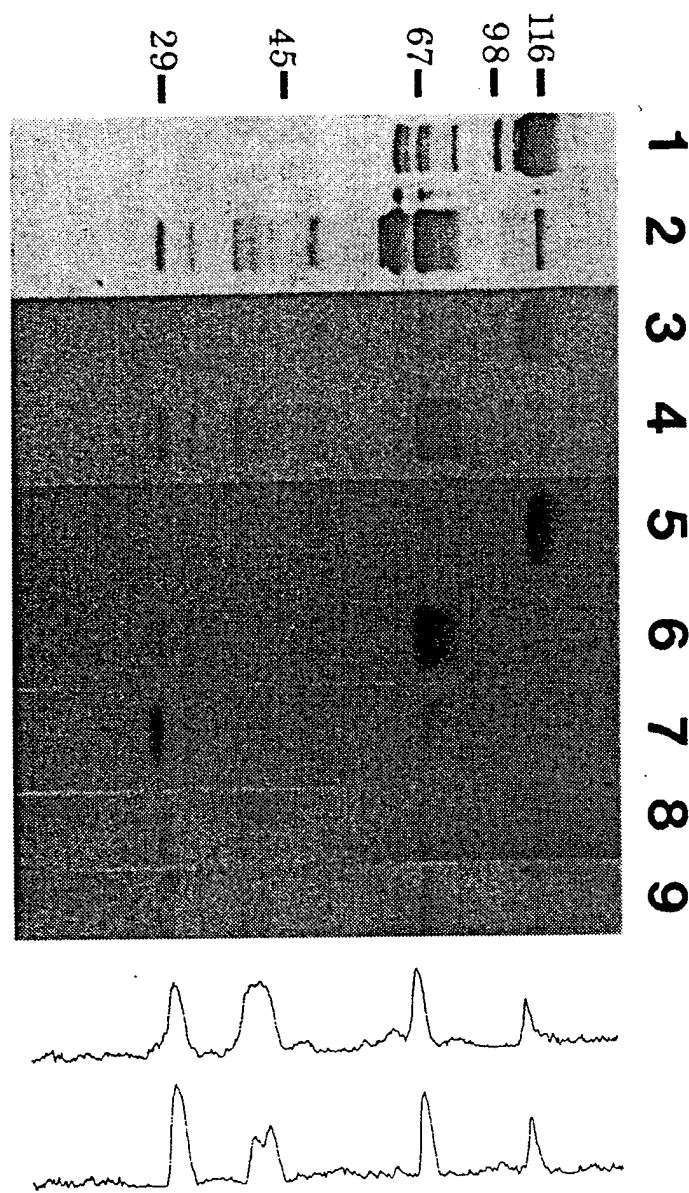
Fig. 7



after electrophoresis on 10% SDS-PAGE and transblot to nitrocellulose membranes followed by Western blot with anti-poly(ADP-ribose) polymerase antiserum (28), as shown in Fig. 8 (Lanes 1,2). The native enzyme protein (Lane 1, Fig. 8) contains traces of polypeptide degradation products of poly(ADP-ribose) polymerase having masses of 98, 80, 67 and 56 kDa (6). As shown in Lane 2 of Fig. 8, digestion of poly(ADP-ribose) polymerase with plasmin (see legend to Fig. 8) yielded 64, 56, 36 and 29 kDa polypeptides (6) and some minor peptides. When these transblotted polypeptides were probed with [¹²⁵I]-labeled poly(ADP-ribose) polymerase for self-binding, the intact poly(ADP-ribose) polymerase, the 64 kDa, the 36 kDa and the 29 kDa polypeptides exhibited strongest binding (Fig. 8, Lanes 3 and 4). The same polypeptides also bound DNA (Fig. 8, Lanes 5 and 6), and the 29 and 64 kDa peptides incorporated [⁶⁵Zn] (Lane 7, Fig. 8). Since it is known that zinc-finger polypeptides of the 29 kDa fragment are required for the binding of DNA termini (27) the role of Zn²⁺ in self-binding of poly(ADP-ribose) polymerase had to be clarified. As illustrated in Fig. 8, (Lanes 8 and 9) zinc-depleted (Lane 8) or zinc-replenished (Lane 9) polypeptides of 64 kDa, 36 kDa and 29 kDa mass equally bound radioiodinated poly(ADP-ribose) polymerase, suggesting that the basic (64 kDa) polypeptide fragment of poly(ADP-ribose) polymerase participates in self-binding and Zn²⁺ may not be critical in this self-association reaction. Densitometric tracings of Lanes 8 and 9 confirm the conclusions deduced from visual inspection of the bands and it is apparent that self-association of poly(ADP-ribose) polymerase at the 64 and 29

Figure 8. Identification of the basic polypeptide domain (64 kDa) as the self-binding portion of poly(ADP-ribose) polymerase Lanes 1 and 2 are immunostained blots of poly(ADP-ribose) polymerase (Lane 1) and its plasmin-digested (Lane 2) polypeptides. Lanes 3 and 4 are autoradiograms of transblotted poly(ADP-ribose) polymerase and its polypeptide fragments, both probed with [¹²⁵I]-labeled poly(ADP-ribose) polymerase. Lanes 5 and 6 are autoradiograms of transblotted poly(ADP-ribose) polymerase and its polypeptide fragments, both probed with [³²P]-labeled DNA. Lane 7 shows two polypeptide fragments (64 and 29 kDa) of poly(ADP-ribose) polymerase labeled with ⁶⁵Zn²⁺. Lanes 8 and 9 are polypeptide fragments of poly(ADP-ribose) polymerase obtained by plasmin digestion of poly(ADP-ribose) polymerase which on nitrocellulose membrane transblots bind [¹²⁵I]-labeled poly(ADP-ribose) polymerase (64, 39, and 29 kDa peptides). The polypeptides shown in Lane 8 contain no Zn²⁺, which was lost during electrophoresis and renatured in the presence of EDTA (see Methods). In lane 9, Zn²⁺ had been reincorporated into polypeptides on nitrocellulose transblots. Both Zn²⁺-free and Zn²⁺-replenished polypeptides bound poly(ADP-ribose) polymerase equally, as shown in the densitometric tracing made from Lanes 8 and 9.

Fig. 8



kDa peptide domains is Zn²⁺ independent. As shown in Fig. 7, the two discrete polypeptide domains specific for histone binding are also part of the 64 kDa proteolytic enzyme fragment.

In further experiments, CNBr-generated peptides were separated by electrophoresis followed by transblot to PVDF membranes and incubation with radioiodinated poly(ADP-ribose) polymerase to detect self-association. This technique identified two discrete poly(ADP-ribose) polymerase-binding polypeptide fragments (separation not shown) and their N-terminal amino acid sequence was: VKTQT... for the 13 kDa fragment (326-445, 120 residues, M_r 13056) and KKTLK... for the 9 kDa fragment (526-606, 81 residues, M_r 9070). The same 13 kDa polypeptide coeluted with the poly(ADP-ribose) polymerase molecule on a Sephadex G75 column as identified by SDS-PAGE (not shown), indicating self-binding in solution. Positioning of the 13 and 9 kDa CNBr fragments together with the histone- binding polypeptides (Fig.7) shows the existence of contiguous and intermittent histone- and self-binding regions in the poly(ADP-ribose) polymerase molecule. The 29 kDa N-terminal polypeptide, which was not further fragmented, comprises the third domain involved in self-association. As stated above, CNBr fragmentation of the 29 kDa polypeptides yielded fragments too small for binding assays in our test system.

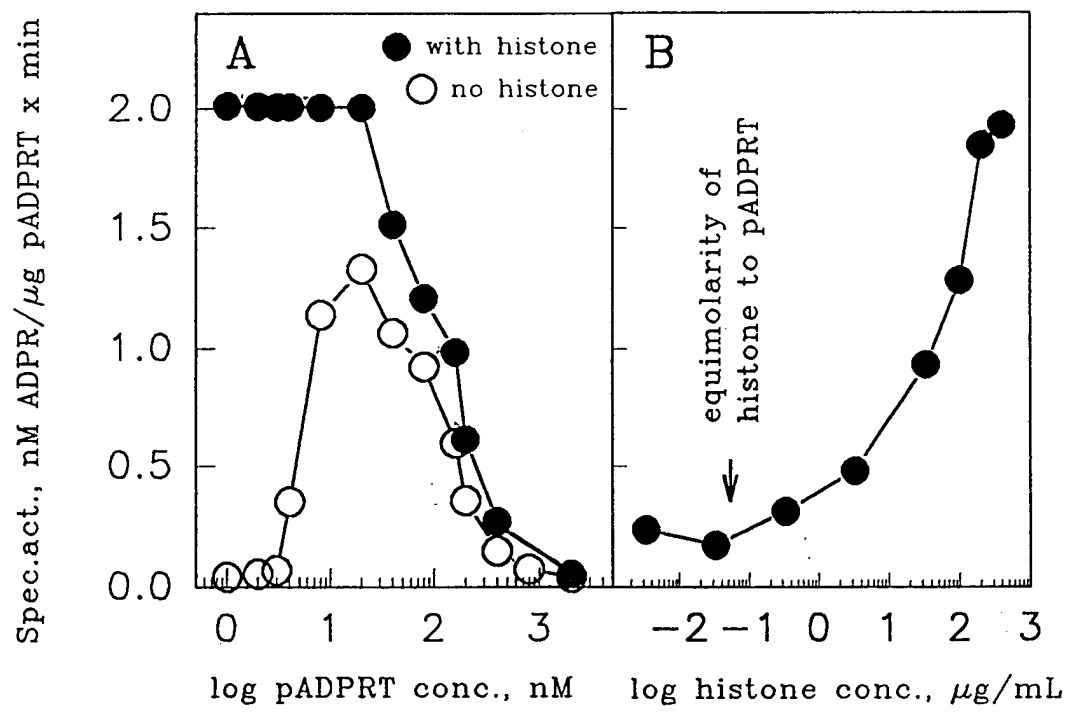
The effect of histone H3 on the enzymatic activity of poly(ADP-ribose)

polymerase. Both the binding of histones to poly(ADP-ribose) polymerase (25) and self-association of the poly(ADP-ribose) polymerase protein (12,13) exert significant stimulation of poly ADP-ribosylation. We therefore devised experiments which can demonstrate a correlation between protein-protein binding, as described above, and the enzymatic activity of poly(ADP-ribose) polymerase. Although all types of histones may behave similarly (24) we studied histone H3 in detail, because this histone was specifically poly-ADP-ribosylated in activated thymocytes (26). As illustrated in Fig. 9A, a protein concentration-dependent association of poly(ADP-ribose) polymerase molecules induces an increase of enzymatic rates between 0 and 30 nM poly(ADP-ribose) polymerase, and at higher enzyme concentrations the specific activity decreases, probably due to inhibitory higher order self-association of the monomers (12). In the presence of histone H3, a dilute - by itself inactive - poly(ADP-ribose) polymerase solution exceeds its maximal polymerase activity assayed in the absence of histone H3. However above 30 nM poly(ADP-ribose) polymerase the specific activity diminishes parallel with the increase of poly(ADP-ribose) polymerase concentration, similar to the behavior of the enzyme in the absence of histone.

Figure 9. The effect of histone H3 on the catalytic activity of poly(ADP-ribose) polymerase. Fig. 9A illustrates the effect of poly(ADP-ribose) polymerase concentration on the specific activity of the enzyme in the absence and presence of histone H3, determined in the presence of 200 μM [^{32}P]-NAD $^+$ and 200 $\mu\text{g}/\text{ml}$ coenzymic DNA. Enzymatic activity of poly(ADP-ribose) polymerase at varying enzyme concentrations was assayed (6, 54) either in the absence (open circles) or in the presence (closed circles) of 200 mg/ml of histone H3 for 1 min at 23°C. The reactions were started by adding 1 ml of poly(ADP-ribose) polymerase to reaction mixtures of varying volumes. The specific activity of the enzyme (ordinate) is plotted against the log of enzyme concentration (abscissa). Fig. 9B shows the effect of varying histone concentration on the specific activity of poly(ADP-ribose) polymerase. The poly(ADP-ribose) polymerase concentration in Fig. 9B was 5.5 nM and the histone concentration varied between 0.03 to 200 mg per ml.

Fig. 9

50



The effect of histones on the chain-length distribution of poly(ADP-ribose). Since direct counting of ^{32}P -labeled $(\text{ADP-RIBOSE})_n$ polymer yields only an indication of enzymatic rates, expressed here as specific activity, we also analyzed the polymer distribution of the product by gel electrophoresis as illustrated in Fig. 10. At low (2 nM) enzyme concentration in the absence of histones mainly branched polymers, as seen at the origin, and long polymers were formed. Addition of histones tend to produce shorter oligomers (Lane 2). Similar observations were made at 20 nM poly(ADP-ribose) polymerase concentration (Lane 3 and 4) and at 200 nM poly(ADP-ribose) polymerase concentration the formation of short oligomers is readily observable (Lanes 5 and 6).

Nucleosomal structure-dependent poly-ADP-ribosylation of histones. The activation of poly(ADP-ribose) polymerase by histone H3 (26) was dependent on histone concentration (Fig. 9B). The most obvious explanation for the activation of poly(ADP-ribose) polymerase by histones would suggest that histone H3 or other histones merely serves as an ADP-ribose acceptor. However, as tested by gel electrophoresis (Line 2 in Fig. 11), only 1 to 5% of poly ADP-ribose was detectable on histone H3 or other histone species and the rest of ADP-ribose oligomers were covalently bound to poly(ADP-ribose) polymerase protein itself, comprising "self-ADP-ribosylation".

The apparent contradiction between these enzymological results and the known poly ADP-ribosylation of histones in nuclei was resolved by

Figure 10. The influence of variation in poly(ADP-ribose) polymerase concentration, in the absence and presence of a constant concentration of mixed histones, on the chain-length distribution of poly(ADP-ribose). The concentrations of poly(ADP-ribose) polymerase in the reaction solution assayed were 2 nM (Lanes 1 and 2), 20 nM (Lanes 3 and 4) and 200 nM (Lanes 5 and 6). Odd numbered solutions contained no histones, even numbered ones contained mixed histone (200 µg/ml). The volumes of the reaction solutions were each 100 µl when the poly(ADP-ribose) polymerase concentrations were 20 and 200 nM, and the volume was 1000 µl when the poly(ADP-ribose) polymerase concentration was 2 nM. The assays were carried out under conditions described in legend to Fig. 9. At the end of incubation for 5 min at 23°C the reaction was stopped with 20% TCA (4°C), the precipitates were sedimented by centrifugation, washed 4 times with 10% TCA (4°C), twice with absolute ethanol (200 µl per wash), and then air-dried and dissolved in 2% SDS containing 10 mM Tris-HCl, 1 mM EDTA, pH 8.0 (50 µl) and 100 µg of proteinase K. Aliquots of the [³²P]-labeled poly(ADP-ribose) representing 30,000 cpm were withdrawn and adjusted to 20 µl with 10 mM Tris-HCl, 1 mM EDTA, pH 8.0, then loaded onto 20% PAGE with TBE as running buffer. Xylene cyanol and bromophenol blue were used as polymer size markers.

Fig. 10

53

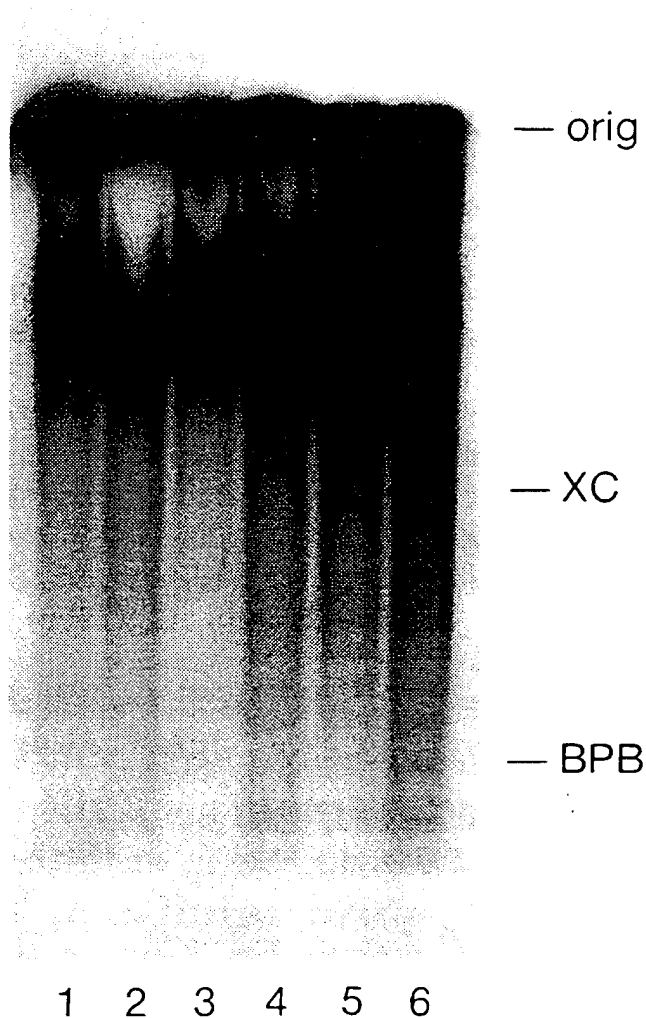
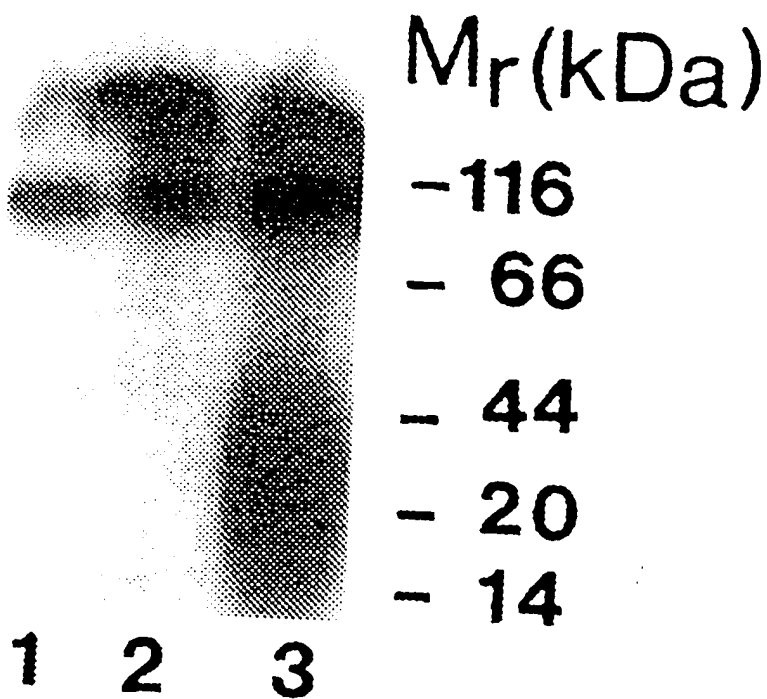


Figure 11. Poly-ADP-ribosylation of poly(ADP-ribose) polymerase and histones in reconstructed nucleosome. Nucleosome reconstruction and assay of poly(ADP-ribose) polymerase activity was done as described in Materials and Methods. Proteins were separated by acidic SDS-PAGE (55). Lane 1, poly(ADP-ribose) polymerase (1.2mg)+ coDNA(10mg); Lane 2, poly(ADP-ribose) polymerase (1.2mg)+ coDNA(10mg) + histone H3(10mg); Lane 3, poly(ADP-ribose) polymerase (1.2mg) + reconstructed nucleosome (equal to 10mg DNA).

Fig. 11

55



demonstrating that artificially reconstructed nucleosomes (40) indeed provided favorable conditions for extensive poly ADP-ribosylation of histones, as illustrated in Fig. 11. In Lane 1 of Fig. 11, auto-ADP-ribosylation of poly(ADP-ribose) polymerase is shown in the presence of DNA. Addition of mixed histones (Lane 2) increased auto-ADP-RIBOSE-ribosylation of poly(ADP-ribose) polymerase without detectable histone ADP-ribosylation. However, in reconstructed nucleosomes extensive poly ADP-ribosylation of histones was apparent (Lane 3, Fig. 11).

Discussion

The previously outlined domain structure of poly(ADP-ribose) polymerase, which consists of DNA binding, self ADP-ribosylation and catalytic domains (31), has now been expanded to include protein- and self-association participating polypeptide regions. Because histones completely block the association of poly(ADP-ribose) polymerase to all proteins (Fig. 1), that in the absence of histones bind poly(ADP-ribose) polymerase, it seems reasonable to postulate that a more detailed analysis of histone binding sites of poly(ADP-ribose) polymerase may be a first approximation to the identification of general protein binding domain of poly(ADP-ribose) polymerase. Our technique of protein-protein binding assays has a size limitation (approximately 6-10 kDa) thus its accuracy is relatively limited. Furthermore binding strength is estimated only by salt gradients sufficient to disrupt association. Despite these shortcomings, our results clearly show that protein-protein binding regions coincide with DNA binding and automodification domains (Fig. 7). Since the DNA-binding zinc-finger region regulates, by as yet unknown mechanisms, the enzymatic as well as DNA binding activities of poly(ADP-ribose) polymerase, the proximity of protein binding sites implies that the two types of macromolecular associations, i.e., protein/DNA and protein/protein interactions, may have mutual regulatory functions, which are clearly of highly complex nature. Since auto-poly-ADP-ribosylation by electrostatic repulsion inhibits poly(ADP-ribose) polymerase-DNA binding (9, 29) and an oscillating poly(ADP-ribosylation) of histones has

been recognized (46), the inhibition of polyADP-riboseibose synthesis - without altering the catabolism of polymers - would be expected to have profound effects on the above outlined macromolecular interactions.

Consistent with this prediction we have observed large cellular phenotypic changes upon treatment of intact cells with specific poly(ADP-ribose) polymerase ligands, reflecting pleiotropic responses (57). A more specific understanding of macromolecular association of poly(ADP-ribose) polymerase requires spectroscopic and fluorometric techniques, implementation of which is now made more feasible by our outline of protein binding domains of this complex protein.

Our results suggests that the presence of Zn^{2+} in the basic polypeptide fragments of poly(ADP-ribose) polymerase appears to be unnecessary for binding to intact poly(ADP-ribose) polymerase. However the presence of Zn^{2+} in the poly(ADP-ribose) polymerase molecule which is used as a binding reagent may weaken this argument since the Zn^{2+} in the intact poly(ADP-ribose) polymerase may not be required for the binding to zinc-free polypeptides. A direct test of this assumption is technically not possible, because removal of Zn^{2+} from poly(ADP-ribose) polymerase by specific reagents (47) results in large changes in the physical properties of poly(ADP-ribose) polymerase that make it experimentally unsuited for binding assays (unpublished results).

Both histone- and self-association have significant influence on the specific polymerase activity of this enzyme (Fig 9), and it appears meaningful that both protein-binding domains reside within the 64 kDa

basic part of the poly(ADP-ribose) polymerase molecule, which also contains DNA binding domains (31), the 29 kDa part with its zinc fingers binding to DNA termini (27) and the 36 kDa part (6) that binds to internal regions of certain double stranded DNAs (48, 49). The effect of histones on the enzymatic activity of poly(ADP-ribose) polymerase is not confined to an action on apparent specific activity, as illustrated at various protein concentrations (Fig. 9). Histones also induce the synthesis of many short chain oligomers (Fig. 10), an observation that agrees with previously obtained results with the carboxyl-terminal domain of human poly(ADP-ribose) polymerase (50). The apparent nonselectivity of histones as poly(ADP-ribose) polymerase-binding proteins is in contrast to the well known specific biological function of histones in the nucleus (43). It has been shown (51) that in isolated polynucleosomes the concentration of NAD⁺ determines the rate of poly-ADP-ribosylation of various histone species, indicating that the concentration of NAD⁺ and the nucleosomal structure, or both, are both regulators of histone-specific poly-ADP-ribosylation. The absence of poly- ADP-ribosylation of histones in solution by purified poly(ADP-ribose) polymerase has been previously reported (52) but the changes in the polymer-accepting function of histones, as a consequence of supramolecular structural modifications, as we have shown here (Fig 11), have not so far been considered. The apparent nonspecificity of histones to bind poly(ADP-ribose) polymerase in our model system appears to be explained by the commonality of lysine-rich polypeptide domains present in all histones (42, 43) as experimentally demonstrated here with proteolytic fragments of histone

H1 (Fig. 3). It has been shown that the free poly(ADP-ribose) polymer binds to lysine-rich histone tails (41), the same domain which associates with specific basic polypeptides of poly(ADP-ribose) polymerase, as documented here for H1. The binding of the acidic poly(ADP-ribose) to lysine-rich polypeptides appears to be explainable by electrostatic forces, but the association of basic polypeptide domains of histones to lysine-rich polypeptides is not consistent with ionic binding and may require hydrophobic mechanisms.

Our results, identifying the 29 kDa and two smaller domains (9 and 13 kDa) of poly(ADP-ribose) polymerase to be participatory in self-association, may be correlated with predictions made from the cDNA structure of poly(ADP-ribose) polymerase isolated from Drosophila (53). A leucine zipper motif has been identified in the automodification domain of the Drosophila enzyme, and it is noteworthy that the amphipathic helix at 395-417 residues of the bovine poly(ADP-ribose) polymerase includes a degenerate "bZip" domain identified in Drosophila (53). The functional importance of this domain in the self-association of poly(ADP-ribose) polymerase appears to be supported by our results.

References

1. Yamanaka, H., Penning, S.A., Willis, E.H., Wasson, D.B. and Carson, D.A. (1988) *J. Biol. Chem.* **263**, 3879-3883.
2. Ludwig, A., Behnke, B., Holtlund, J. and Hilz, H. (1988) *J. Biol. Chem.* **263**, 6993-6999.
3. Kirsten, E., Bauer, P.I. and Kun, E. (1991) *Exp. Cell Res.* **194**, 1-8.
4. Bauer, P.I. and Kun, E. (1985) in ADP-ribosylation of Proteins (Althaus, F.R., Hilz, H. and Shall, S. Eds.) pp. 63-74, Springer-Verlag, Berlin.
5. Simonin, F., Ménissier-de Murcia, J-M., Poch, O., Muller, S., Gradwohl, G., Molinete, M., Penning, C., Keith, G. and de Murcia, G. (1990) *J. Biol. Chem.* **256**, 19249-19256.
6. Buki, K.G. and Kun, E. (1988) *Biochemistry* **27**, 5990-5995.
7. Cole, A.G., Bauer, G., Kirsten, E., Mendeleyev, J., Bauer, P.I., Buki, K.G., Hakam, A. and Kun, E. (1991) *Biochim. Biophys. Res. Commun.* **180**, 504-514.

8. Simbulan, C-M. G., Suzuki, M., Izuta, S., Sakurai, T., Savoysky, E., Miyahara, K., Shizuta, Y. and Yoshida, S. (1993) *J. Biol. Chem.* **268**, 93-99.
9. Buki, K.G., Bauer, P.I. and Kun, E. (1991) *Biochem. Biophys. Res. Commun.* **180**, 496-503.
10. Satoh, M.S. and Lindahl, T. (1992) *Nature* **356**, 356-358.
11. Satoh, M.S., Poirier, G.G. and Lindahl, T. (1993) *J. Biol. Chem.* **268**, 5480-5487.
12. Bauer, P.I., Buki, K.G. and Kun, E. (1990) *Biochem. J.* **270**, 17-26.
13. Mendoza-Alvarez, H. and Alvarez-Gonzales, R. (1993) *J. Biol. Chem.* **68**, 22575-22580.
14. Bauer, P.I., Hakam, A. and Kun, E. (1986) *FEBS Lett.* **195**, 331-338.
15. Yoshihara, K., Tanigawa, Y., Bruzio, L. and Koide, S.S. (1975) *Proc. Natl. Acad. Sci. USA* **72**, 289-293.
16. Yoshihara, K., Itaya, A., Tanaka, Y., Ohashi, Y., Ito, K., Teroaka, H., Tsukada, K., Matsukage, A. and Kamiya, T. (1985) *Biochem. Biophys. Res. Commun.* **128**, 61-67.

17. Ohashi, Y., Itaya, A., Tanaka, Y., Yoshihara, K., Kamiya, T. and Matsukage, A. 1986) Biochem. Biophys. Res. Commun. **140**, 667-673.
18. Ferro, A.M. and Olivera, B.M. (1984) J. Biol. Chem. **259**, 547-554.
19. Kasid, U.N., Halligan, B., Lieu, L.F., Dritschilo, A. and Smulson, M. (1989) J. Biol. Chem. **264**, 18687-18692.
20. Darby, M.K., Schmitt, B., Jongstra-Bilen, J. and Vosberg, H-P. (1985) EMBO J. **4**, 2129-2134.
21. Rice, W.G., Hillyer, C.D., Harten, B., Schaeffer, C.A., Dorminy, M., Lackey III, Kirsten, E., Mendeleyev, J., Buki, K.G., Hakam, A., and Kun, E. (1992) Proc. Natl. Acad. Sci. USA **89**, 7703-7707.
22. Ueda, K. and Hayaishi, O. (1985) Ann. Rev. Biochem. **54**, 73-100.
23. Minaga, T., Romaschin, A., Kirsten, E. and Kun, E. (1979) J. Biol. Chem. **254**, 9663-9668.
24. Boulikas, T. (1988) EMBO J. **7**, 57-67.
25. Yoshihara, K. (1972) Biochem. Biophys. Res. Commun. **47**, 119-125.

26. Sooki-Toth, A., Banfalvi, G., Szollosi, J., Kirsten, E., Antoni, F. and Kun, E. (1989) *Exp. Cell Res.* **184**, 44-52.
27. Gradwohl, G., Ménissier-de Murcia, J., Molinete, M., Simonin, F., Koken, M., Hoeijmakers, J. H. J. and de Murcia, G. (1990) *Proc. Natl. Acad. Sci. USA* **87**, 2990-2994.
28. Buki, K.G., Kirsten, E. and Kun, E. (1987) *Anal. Biochem.* **167**, 160-167.
29. Buki, K.G., Bauer, P.I., Mendeleyev, J., Hakam, A. and Kun, E. (1991) *FEBS Lett.* **290**, 181-185.
30. Laemmli, U.K. (1970) *Nature* **227**, 680-685.
31. Kameshita, I., Matsuda, Z., Taniguchi, T. and Shizuta, Y. (1984) *J. Biol. Chem.* **259**, 4770-4776,
32. Simonin, F., Briand, J.-P., Muller, S. and de Murcia, G. (1991) *Anal. Biochem.* **195**, 226-231.
33. Hartman, P.G., Chapman, G.E., Moss, T. and Bradbury, E.M. (1977) *Eur. J. Biochem.* **77**, 45-51.

34. Bradbury, E.M., Chapman, G.E., Danby, S.E., Hartman, P.G. and Riches, P.L. (1975) *Eur. J. Biochem.* **57**, 521-528.
35. Ausubel, F.M., Brent, R., Kongston, R.E., More, D.D., Seidman, J.G. Smith, J.A. and Struhl, K., eds., *Current Protocols in Molecular Biology*, Wiley Interscience, 1987. p3.5.7.
36. Schägger, H. and von Jagow, G. (1987) *Anal. Biochem.* **166**, 368-379.
37. Hunkapiller, M.W., Hewick, K.M., Dreyer, W.J. and Hood, L.E. (1983) *Methods in Enzymol.* **91**, 399-413.
38. Ball, E.H. (1986) *Anal. Biochem.* **155**, 23-27.
39. Naegli, H. and Althaus, F.R. (1991) *J. Biol. Chem.* **266**, 10596-10601.
40. Stein, A. (1987) *J.Biol. Chem.* **262**, 3872-3879.
41. Panzeter, P.L., Zweitel, B., Malagna, M., Waser, S.H., Richard, M-C. and Althaus, F.R. (1993) *J. Biol. Chem.* **268**, 17662-17664.
42. Isenberg, I. (1979) *Ann. Rev. Biochem* **48**, 151-191.
43. Wolffe, A.P. (1994) *Cell* **77**, 13-16.

44. Saito, I., Hatakeyama, K., Kido, T., Ohkubo, H., Nakanishi, S. and Ueda, K. (1990) *Gene* **90**, 249-254.
45. Shizuta, Y., Kameshita, I., Agemori, M., Ushiro, H., Taniguchi, T., Otsuki, M., Sekimizu, K. and Natori, S. (1985) in ADP-Ribosylation of Proteins (Althaus, F. R., Hilz, H. and Shall, S. eds.) pp.52-59. Springer-Verlag, Berlin.
46. Althaus, F.R. (1992) *J. Cell Sci.* **102**, 663-670.
47. Rice, W.R., Schaeffer, C.A., Harten, B., Villinger, F., South, T.L., Summers, M.F., Henderson, L.E., Bess, Jr., J.W., Arthur, L.O., McDougal, J.S., Orloff, S.L., Mendeleyev, J. and Kun, E. (1993) *Nature*, **361**, 473-475.
48. Sastry, S.S., Buki, K.G. and Kun, E. (1989) *Biochemistry* **28**, 5670-5680 .
49. Sastry, S.S. and Kun, E. (1990) *Biochem. Biophys. Res. Commun.* **167**, 842-847.
50. Simonin, F., Höfferer, L., Panzeter, P.L., Muller, S., de Murcia, G. and Althaus, F.R. (1993) *J. Biol. Chem.* **268**, 13454-13461.

51. Huletsky, A., Niedergang, C., Fréchette, A., Aubin, R., Gaudreau, A. and Poirier, G.G. (1985) Eur. J. Biochem. **146**, 277-285.
52. Ikejima, M., Marsischky, G. and Gill, D.M. (1987) J. Biol. Chem. **262**, 17641-17650.
53. Uchida, K., Hanai, S., Ishikawa, K., Ozawa, Y, Uchida, M., Sugimura, T. and Miwa, M. (1993) Proc. Natl. Acad. Sci. USA **90**, 3481-3485.
54. Hakam, A., McLick, J., Buki, K.G. and Kun, E. (1987) FEBS Lett. **212**, 73-78.
55. Jackowski, G. and Kun, E. (1983) J. Biol. Chem. **258**, 12587-12593.
56. Molinete, M., Schreiber, V., Simonin, F., Gradwohl, G., Delarue, M., Ménissier-de Murcia, J-M. and de Murcia, G. Abstract 8 in the "Oji International Seminar on ADP-ribosylation Reactions", Sept. 23-26, 1992, Tsukuba, Japan.
57. Young, L.J.T. and Kun, E. Abstract 112 in the "The 11th International Symposium on ADP-ribosylation: DNA Repair, Signal Transduction", September 17-21, 1994, Strasbourg-Bischberg, France.

Reversion of malignant phenotype by 5-iodo-6-amino-1,2-benzopyrone, a noncovalently binding ligand of poly(ADP-ribose) polymerase

Summary

A noncovalently binding inhibitory ligand of poly(ADP-ribose) polymerase, 5-iodo-6-amino-1,2-benzopyrone, when incubated at 5-600 μ M external concentration with an E-ras-transformed tumorigenic cell line or with human prostatic carcinoma cells for 4 to 6 days converts both cancer cells to a nontumorigenic phenotype that is characterized by drastic changes in cell morphology, absence of tumorigenicity in nude mice, and a high rate of aerobic glycolysis.

Introduction

A noncovalently binding ligand of poly(ADP-ribose) polymerase, 1,2-benzopyrone, when administered to rats inhibited *in vivo* tumorigenesis by a dexamethasone activation sensitive ras gene construct containing tumorigenic transformed rat cell line (1). Substitution of an amino group in the 6- position of 1,2-benzopyrone, resulting in 6-amino-1,2-benzopyrone, significantly increased the cytostatic activity of this molecule (2). Additional substitution with iodine in position 5, yielding 5-iodo-6-amino-1,2-benzopyrone, increased by at least two orders of magnitude the cellular inhibitory potency of this molecule towards poly(ADP-ribose) polymerase assayed in permeabilized cells. Because of the high enzyme inhibitory potency and selectivity ($I_{50} = 10 \mu\text{M}$) and the low apparent *in vivo* toxicity of this compound (150 mg/kg, i.p. in rats had no toxic effect) we tested the effect of pretreatment of tumorigenic cells with 5-iodo-6-amino-1,2-benzopyrone on the rate of tumor development in immunodeficient nude mice. Two tumorigenic cell lines were chosen, one an E-ras-transformed bovine endothelial cell line and the second a human prostatic carcinoma cell line, DU 145. The present report describes the abolishment of tumorigenicity of both cancer cells by relatively brief (6-20 days) pretreatment of cells with 5-600 μM 5-iodo-6-amino-1,2-benzopyrone.

Materials and Methods

Primary cultures of bovine endothelial cells were transformed by Ha-ras gene present in pSV2neo24 plasmid and repeated stimulation with 50 μ M thrombin. The transformed cells were isolated by clonal selection in the presence of 250 μ g/ml of G418. Detailed characterization of the highly malignant E-ras 20 cell line will be reported elsewhere (P.I. Bauer, G. Mikala, G. Varadi, E. Csonka, K.G. Buki, L.J.T. Young, J.A. Comstock, E. Kirsten, J. Mendeleyev, A. Hakam and E. Kun, manuscript in preparation). E-ras 20 cells were cultured in Dulbecco MEM + 10% FCS and seeded for cell growth assays at a density of 35,000 cells per cm^3 . 5-iodo-6-amino-1,2-benzopyrone was added in DMSO at a final concentration of 5-600 μ M. Cell count, morphology and DNA synthesis (1,2) were monitored from 1-6 days, when tumorigenicity was assayed by s.c. injection of 10^5 cells in nude mice. Aerobic glycolysis was assayed in a microphysiometer (3). Prostatic cancer cells (DU-145) were cultured in PME and treated with 600 μ M 5-iodo-6-amino-1,2-benzopyrone for 6 to 20 days prior to tumorigenicity assay (10^6 cells per s.c. injection).

Results and Discussion

As shown in Fig. 1, treatment of E-ras 20 cells with 5-iodo-6-amino-1,2-benzopyrone at concentrations ranging from 300-600 μM produced large morphologic changes, coinciding with significant cytostasis, but no immediate cell death. At 5-600 μM drug the morphological transformation was maximal and could be already detected 3-4 hours after the addition of the drug. A nontumorigenic transformed cell line was obtained after treatment for 5-6 days which sustained its transformed phenotype in the presence of the drug, then progressively died after 10-12 days. The same transformation of E-ras 20 cells to the nontumorigenic phenotype was obtained also by 0.3 mM 5-iodo-6-amino-1,2-benzopyrone but a pretreatment for 40 days was required. The morphologic changes in E-ras 20 cells induced by 600 μM 5-iodo-6-amino-1,2-benzopyrone for 6 days is shown in Fig.1.

Subcutaneous injection of 10^5 E-ras 20 cells into nude mice produced after 4-5 days latency rapidly growing fibrosarcomas, whereas cells pretreated with 500 μM 5-iodo-6-amino-1,2-benzopyrone produced no tumors at all (Fig. 2). Tumorigenicity of E-ras 20 cells and its repression by 5-iodo-6-amino-1,2-benzopyrone treatment illustrated in Fig. 2.

Figure 1. Microscopic picture of E-ras 20 (top) and 6-days 5-iodo-6-amino-1,2-benzopyrone-treated induced cell transformants (bottom). Magnification 250X. The transformants are characterized by large cytoplasmic enlargement, cells exhibit contact inhibition and are nontumorigenic (Fig. 2) even after removal of drug and culturing in the absence of drug for two weeks, when cells died by senescent-induced apoptosis.

Fig 1

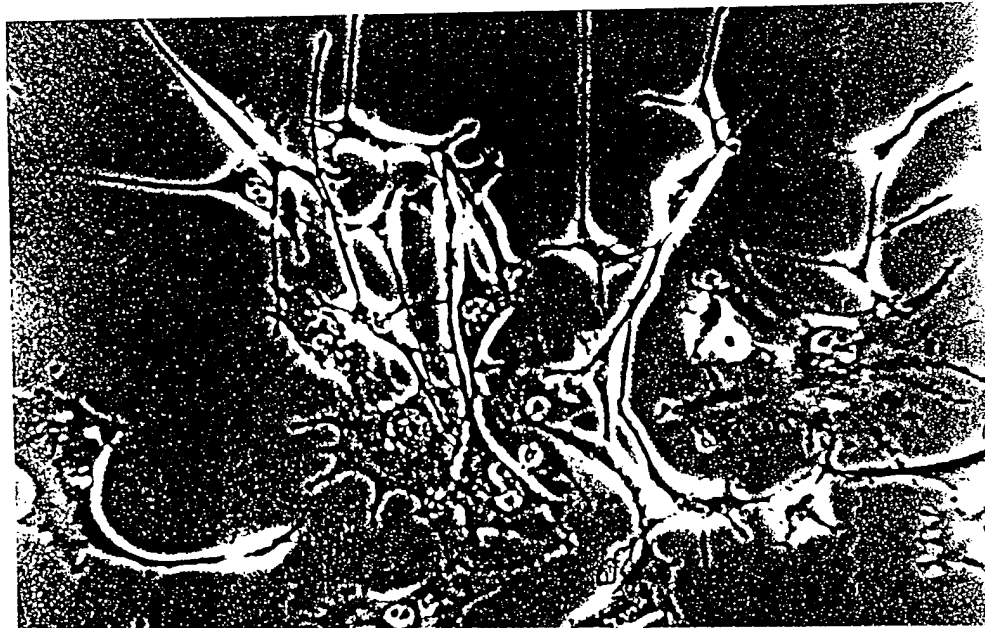
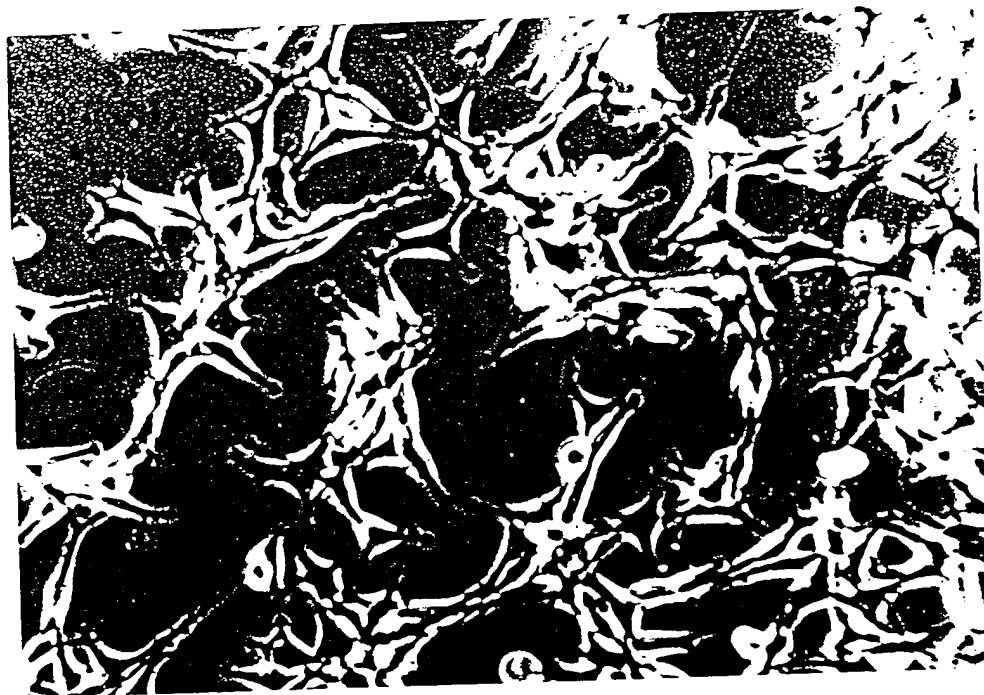
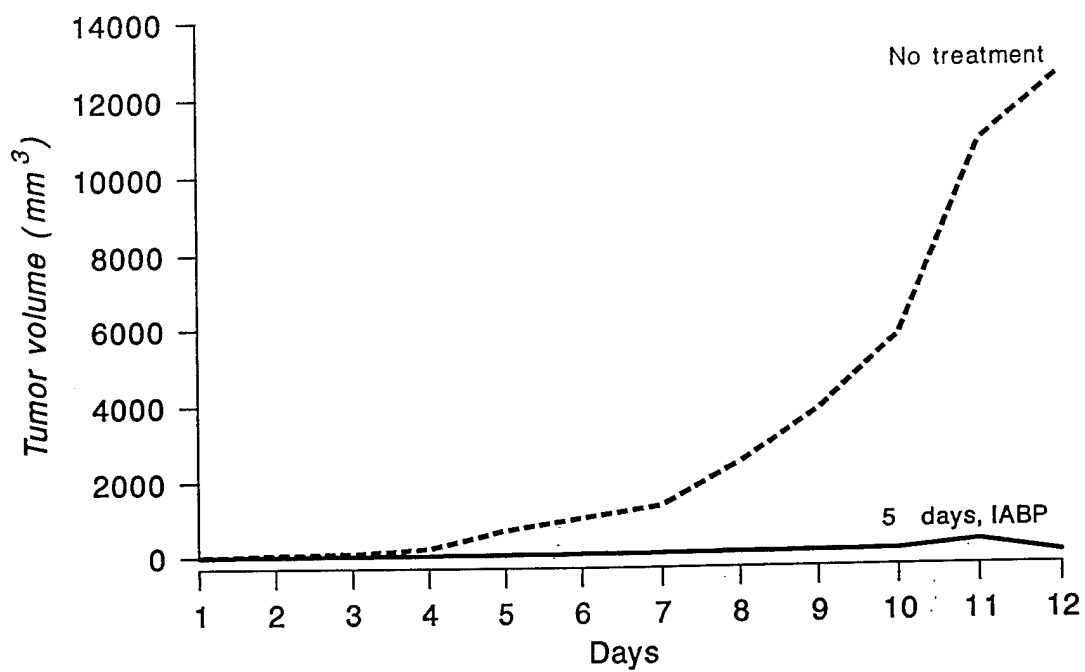


Figure 2. 10^5 E-ras cells were injected s.c. into nude mice and the development of tumor (fibrosarcoma) followed by optical tumor mass measurement. Top curve: No drug pretreatment, bottom curve: absence of tumors induced by 5-days long pretreatment of E-ras 20 cells with 500 μM 5-iodo-6-amino-1,2-benzopyrone.

Fig 2

76



The metabolic phenotype of drug-transformed nontumorigenic cells is illustrated in the Table, which is a kinetic assay for aerobic glycolysis. The enlarged nontumorigenic transformants exhibited a 2 to 2.5 fold increase in glucose metabolism, and this effect was not due to uncoupling of oxidative phosphorylation but to an increase in glycolytic enzyme content.

Injection of 106 DU-145 human prostatic cancer cells produced prostatic adenocarcinomas in nude mice, and pretreatment with 600 μ M 5-iodo-6-amino-1,2-benzopyrone for 6 days completely suppressed tumorigenicity as shown in Fig. 3. Tumorigenicity of DU-145 cells and its inhibition by 5-iodo-6-amino-1,2-benzopyrone pretreatment is demonstrated in Fig. 3.

The transforming effect of 5-iodo-6-amino-1,2-benzopyrone on tumorigenic cells, converting them to a nonmalignant phenotype, appears to be oncogene-nonspecific and can be demonstrated with a wide variety of tumors. In the transformed nontumorigenic cells originating from E-ras 20 cells, the expression of the ras oncogene was completely abrogated but neither the enzyme content of poly(ADP-ribose) polymerase nor the expression of the poly(ADP-ribose) polymerase gene were influenced by the treatment with 5-iodo-6-amino-1,2-benzopyrone. The genomic form of the ras gene was detectable in both E-ras 20 cells and drug-treated nontumorigenic transformants, thus this effect is equivalent to a silencing of ras gene expression.

TABLE

Increased aerobic glycolysis of nontumorigenic transformants

Time (hrs)	*E-ras 20	*Drug-treated transformants
0.6	1.0	2.0
1.1	1.4	4.0
1.9	2.2	8.2
2.5	4.0	10.5
3.0	5.0	14.0

* $\times 10^{10}$ protons per cell (SD = $\pm 2\%$). The effect of treatment with 5-iodo-6-amino-1,2-benzopyrone on proton production by glycolysis in E-ras 20 cells. The E-ras 20 cells were pretreated for 7-days with 0.6 mM 5-iodo-6-amino-1,2-benzopyrone in DMEN growth medium. The acidification rates of harvested cells were measured in a microphysiometer (4) during perfusion with unbuffered DMEN medium with no drug present. During the measurement of proton formation, flow rate was 10 $\mu\text{l}/\text{min}$ and acidification rates ($\mu\text{V}/\text{sec}$) were sampled during a 30 second frame in each 3-min pump cycle of continuous 4-hr experiment. By means of a computer conversion routine, the data were calculated as cumulative proton production per cell.

Figure 3. 10^6 human prostatic adenocarcinoma cells (DU-145) were injected s.c. into nude mice and tumorigenesis was monitored by volume analysis (top curve). Pretreatment of DU-145 cells for 5-days with 600 μ M 5-iodo-6-amino-1,2-benzopyrone abolished tumorigenesis as seen in lower curve.

The only enzyme inhibition detected was that of poly(ADP-ribose) polymerase, but enzyme components of significant signal pathways (e.g. DNA methyl-transferase, protein kinase C, ornithine decarboxylase) are significantly depressed by de-ADP-ribosylated poly(ADP-ribose) polymerase binding to DNA sites which also inhibit DNA synthesis (2). Details of this mechanism will be published elsewhere.

REFERENCES

1. Tseng, A., Jr., Lee, W.F.M., Kirsten, E., Hakam, A., McLick, J., Buki, K., Kun, E. (1987) Prevention of tumorigenesis of oncogene-transformed rat fibroblasts with DNA-site inhibitors of poly(ADP-ribose) polymerase. *Proc. Nat. Acad. Sci. USA* **84**, 1107- 1111.
2. Kirsten, E., Bauer, P.I., Kun, E. (1991) Suppression of dexamethasone-stimulated DNA synthesis in an oncogene construct containing rat cell line by a DNA site-oriented ligand of poly-ADP-ribose polymerase: 6-amino-1,2-benzopyrone. *Exper. Cell Res.* **193**, 1-4.
3. Parce, J.W., Owicky, J.C., Kercso, K.M., Sigal, G.B., Wada, H.G., Muir, V.C., Bousse, L.J., Ross, K.L., Sikic, B.I. and McConnel, H. M. (1989) Detection of cell-affecting agents with a silicon biosensor. *Science* **246**: 181-185 .

**PHOSPHORYLATION OF POLY(ADP-RIBOSE)
POLYMERASE PROTEIN IN HUMAN PERIPHERAL
LYMPHOCYTES STIMULATED WITH PHYTO-
HEMAGGLUTININ**

Summary

Intracellular phosphorylation of poly(ADP-ribose) polymerase was assayed in streptolysin-O-permeabilized human lymphocytes. Whereas ^{32}P incorporation from [γ - ^{32}P]ATP into immuno-precipitated enzyme protein was undetectable in resting cells, significant phosphorylation of this enzyme was observed in lymphocytes treated with phytohemagglutinin. The phosphorylation of poly(ADP-ribose) polymerase in permeabilized cells was not stimulated by phorbol ester, but phosphorylation of other proteins and of a specific oligopeptide substrate of protein kinase C was increased by phorbol ester. The specific inhibitory pseudosubstrate peptide of protein kinase C blocked the phosphorylation of poly(ADP-ribose) polymerase induced by phytohemagglutinin. A potential role of a member of the protein kinase C family in the intracellular regulation of poly(ADP-ribose) polymerase by phosphorylation appears probable.

Introduction

In vitro experiments with purified enzymes have revealed that poly(ADP-ribose) polymerase (EC 2.4.2.30) is inactivated by phosphorylation catalyzed by protein kinase C (1). We have found that simultaneously with the phosphorylation of the polypeptide chain at two different sites, poly(ADP-ribose) polymerase also loses its propensity to bind DNA and added DNA inhibits the phosphorylation of poly(ADP-ribose) polymerase by protein kinase C (2). Thus protein kinase C may control both catalytic and colligative activities of this abundant nuclear protein which in turn influences chromatin structure and gene function (3). However, *in vitro* enzymatic models are insufficient proofs of existing cellular mechanisms. In the present work resting and mitogen-stimulated human lymphocytes served as a model system for the testing of the hypothesis that proposes a connection between protein phosphorylation and intracellular poly(ADP-ribose) polymerase activity.

The idea of application of phytohemagglutinin, a nonphysiological stimulant of lymphocyte proliferation, for the study of the cellular role of poly(ADP-ribose) polymerase has an unusual background. It is known that the propagation of immunodeficiency virus in human lymphocytes *in vitro* requires stimulation by phytohemagglutinin and the inactivation of both retroviral *gag* protein zinc fingers and those of poly(ADP-ribose) polymerase by specific drugs abrogates human immunodeficiency virus proliferation (4,5). Furthermore, phytohemagglutinin stimulates

poly(ADP-ribose) polymerase mRNA production (6) and increases the *de novo* synthesis of poly(ADP-ribose) polymerase in S phase (7). We presumed that a transient and probably reversible inactivation of poly(ADP-ribose) polymerase, induced by phosphorylation, might have a regulatory role in the course of cell proliferation. Here we demonstrate that phytohemagglutinin stimulates also the phosphorylation of poly(ADP-ribose) polymerase in permeabilized whole cells.

Materials and Methods

Human blood lymphocytes were maintained in RPMI 1640, supplemented with 10% fetal calf serum, 2 mM L-glutamine (all from Gibco), 50 IU penicillin and 50 µg/ml streptomycin, at 37 °C, in humidified air containing 5% CO₂.

Peripheral blood was collected from healthy volunteers. Mononuclear cells separated on Ficoll-Iodamide (Pharmacia, Uppsala, Sweden and Bracco, Milano, Italy) gradient by the method of Boyum (8), washed twice and cultured at 10⁶ cells/ml density. Mitogen stimulation was achieved by purified phytohemagglutinin (Wellcome Diagnostics, Dartford, England) at 1 µg/ml concentration. Control samples were maintained at suboptimal stimulation by 0.03 µg/ml phytohemagglutinin. Cells were harvested after treatment for 16-60 h, pelleted by low speed centrifugation (1500 x g, 10 min) to eliminate cell debris, resuspended in RPMI 1640 and viable cells were separated on a Ficoll-Iodamide gradient. Viability was always higher than 94% determined by propidium iodide (Sigma, USA) dye exclusion and light scattering in a flow cytometer (Cytoron Absolute, Ortho Diagnostic System, Raritan, NJ, USA).

Cell count, blast cell content and cell-cycle stages were assayed in a flow cytometer. For cell-cycle measurement samples containing 100 µl

cell suspension from the original cultures were diluted with 900 μ l lysis solution (0.1% v/v Triton X-100 and 0.1% w/v Na-citrate in water) (9), and propidium iodide (20 μ g/ml final concentration) was then added and the suspension incubated at room temperature for 10 min before analysis. Percentages of cells in different cell-cycle phases were evaluated by the software of Cytoron Absolute.

Permeabilization of cells by streptolysin-O was carried out according to the method described by Alexander et al. (10) with minor modifications and the phosphorylation of intracellular proteins was performed in the medium used for permeabilization. The final concentration of components in this medium were 8 mM MgCl₂, 120 mM KCl, 12 mM Hepes (pH 7.4), 10 mM EGTA, 0.5 μ M free Ca²⁺, 0.1 mM [γ -³²P]ATP (about 10⁵ cpm/nmol) and 0.8 U/ml streptolysin-O freshly reconstituted from freeze-dried powder. Cells were incubated in the streptolysin-O containing medium (3 x 10⁶ cells in 0.3 ml medium) for 12 min at 37 °C. At the end of the incubation about 90% of the cells appeared to be permeabilized on the basis of staining with trypan blue. After 12 min incubation the cells were centrifuged (1500 x g, 2 min) and the pellet used for immunoprecipitation of poly(ADP-ribose) polymerase. In some other experiments the incubation was stopped by adding trichloroacetic acid (5% w/v final concentration) and after centrifugation the pellet was subjected to SDS-PAGE on 12% polyacrylamide gels and the phosphoprotein pattern was detected by autoradiography.

Immunoprecipitation (11) was carried out immediately after phosphorylation. After centrifugation the supernatant of cells was carefully removed and the cells lysed in 100 µl of lysis buffer composed of 50 mM Tris-HCl (pH 7.5), 0.1% SDS, 1% NP-40 (Nonidet P-40), 0.5 M NaCl, 1 µg/ml aprotinin and 10 µg/ml phenylmethylsulphonyl fluoride, for one h at 4 °C. Then 400 µl of NET buffer (50 mM Tris-HCl, pH 7.5, 0.1% v/v NP-40, 0.4 M NaCl, 1 mM EDTA, 0.25% w/v gelatin) was admixed and the solution cleared by centrifugation (12000 x g, 5 min) at 4 °C. The samples were incubated with 3 µl/assay (see above) of the antibody, specific for the poly(ADP-ribose) polymerase protein (12), for 3 h at 4 °C followed by an overnight incubation in the presence of protein A-Agarose (Oncogene Sci., 50 µl slurry/tube). The unbound compounds were removed by subsequent washings (4 times with NET buffer, once with Tris-HCl buffer (pH 8.0), containing 1 mM EDTA ; 0.4 ml each wash). Finally the resin was boiled with 50 µl of Laemmli sample buffer for 10 min and 40-µl aliquots from the supernatant of the centrifuged samples were loaded onto 10% SDS-PAGE gels. After electrophoresis gels were stained with coomassie brilliant blue, destained, dried and autoradiographed.

Intracellular protein kinase C activity was checked with the aid of the selective oligopeptide substrate of protein kinase C Ala-Ala-Ala-Ser-Phe-Lys-Ala-Lys-Lys-amide (13,14). Aliquots of cells were incubated for 10 min at 37 °C in the absence or presence of 40 ng/ml phorbol myristyl acetate (Sigma) and the cells were then pelleted and resuspended in the

medium used for permeabilization. Samples (10^6 cells in 100 μ l medium) were permeabilized and incubated in the absence or presence of the oligopeptide (0.7 mg/ml) for 12 min and the incubation stopped with ice-cold glacial acetic acid (0.4 ml). After centrifugation (10000 x g, 2 min) aliquots were taken from the supernatant and the radioactivity of ^{32}P incorporated into the oligopeptide was measured as described previously (13,14). All assays were performed in duplicate. The activation caused by phorbol myristyl acetate was expressed as the difference between the amounts of phosphate incorporated into the oligopeptide in cell samples incubated in the presence and absence of phorbol myristyl acetate.

Poly(ADP-ribose) polymerase and protein kinase C (type II, β) were purified as described previously (15,16). The cyclin-dependent kinase 1-*cdc2* was obtained from UBI (USA) and the protein kinase C pseudosubstrate prototope inhibitory peptide was a generous gift of Dr. Doreen Cantrell (Imperial Cancer Research Fund, London). Phosphorylation of the purified poly(ADP-ribose) polymerase protein was performed as described previously (2).

Results

Intracellular phosphorylation of poly(ADP-ribose) polymerase was studied in human peripheral blood lymphocytes permeabilized by streptolysin-O. In our preliminary experiments the phosphorylation of poly(ADP-ribose) polymerase was not detectable in granulocytes or in resting lymphocytes, therefore we attempted to demonstrate the phosphorylation in artificially induced proliferating cells. Fig. 1 shows that in lymphocytes stimulated by phytohemagglutinin the poly(ADP-ribose) polymerase protein is phosphorylated. As shown previously *in vitro* poly(ADP-ribose) polymerase is a good substrate for type II (β) and type III (α) isoenzymes of protein kinase C (2). Since these isoenzymes are present in lymphocytes (17), we presumed that the phosphorylation in permeabilized cells was catalyzed by protein kinase C. However, when protein kinase C was activated by treatment of resting cells with phorbol myristyl acetate no phosphorylation of poly(ADP-ribose) polymerase could be observed (Fig. 1A). At the same time the phorbol myristyl acetate-induced activation of protein kinase C was demonstrated by the phosphorylation of a number of other intracellular proteins, among them an about 116 kDa protein which on the basis of immunoprecipitation was not identical to poly(ADP-ribose) polymerase (Fig. 2). The intensity of ^{32}P incorporation into the poly(ADP-ribose) polymerase protein was not increased when phytohemagglutinin stimulated cells were further treated with phorbol myristyl acetate (Fig. 1A) although the effect of phorbol

Figure 1. Phosphorylation of poly(ADP-ribose) polymerase in phytohemagglutinin-treated blood lymphocytes. poly(ADP-ribose) polymerase protein was separated from lymphocytes by immunoprecipitation followed by SDS-PAGE and the phosphorylation was detected by the autoradiography of the ^{32}P -labeled band of poly(ADP-ribose) polymerase. Lanes 1-4 of Figure A show the results of control experiments in which samples of purified poly(ADP-ribose) polymerase were phosphorylated *in vitro* by protein kinase C type II (β) isoenzyme. Lanes 1 and 2 of Figure A show the band of *in vitro* phosphorylated poly(ADP-ribose) polymerase without immunoprecipitation, in lane 2 ^{32}P -labeled sample was mixed with 3 μg unlabeled poly(ADP-ribose) polymerase. Lane 3 shows a ^{32}P -labeled sample added to permeabilized control (resting) lymphocytes, lane 4 shows a ^{32}P -labeled sample mixed with 3 μg unlabeled poly(ADP-ribose) polymerase and added to permeabilized control lymphocytes. Lanes 5-8 show the phosphorylation of poly(ADP-ribose) polymerase in permeabilized cells. Control cells (lanes 5,6) and cells stimulated by phytohemagglutinin for 60 h (lanes 7,8) were permeabilized in the absence (lanes 5,7) or presence (lanes 6,8) of 40 ng/ml phorbol myristyl acetate. Lane 2 in Figure B shows the phosphorylation of poly(ADP-ribose) polymerase in cells stimulated by phytohemagglutinin for 16 h, lanes 1 and 3 are identical samples from control cells and lane 4 shows the band of poly(ADP-ribose) polymerase phosphorylated *in vitro*.

93

Fig 1

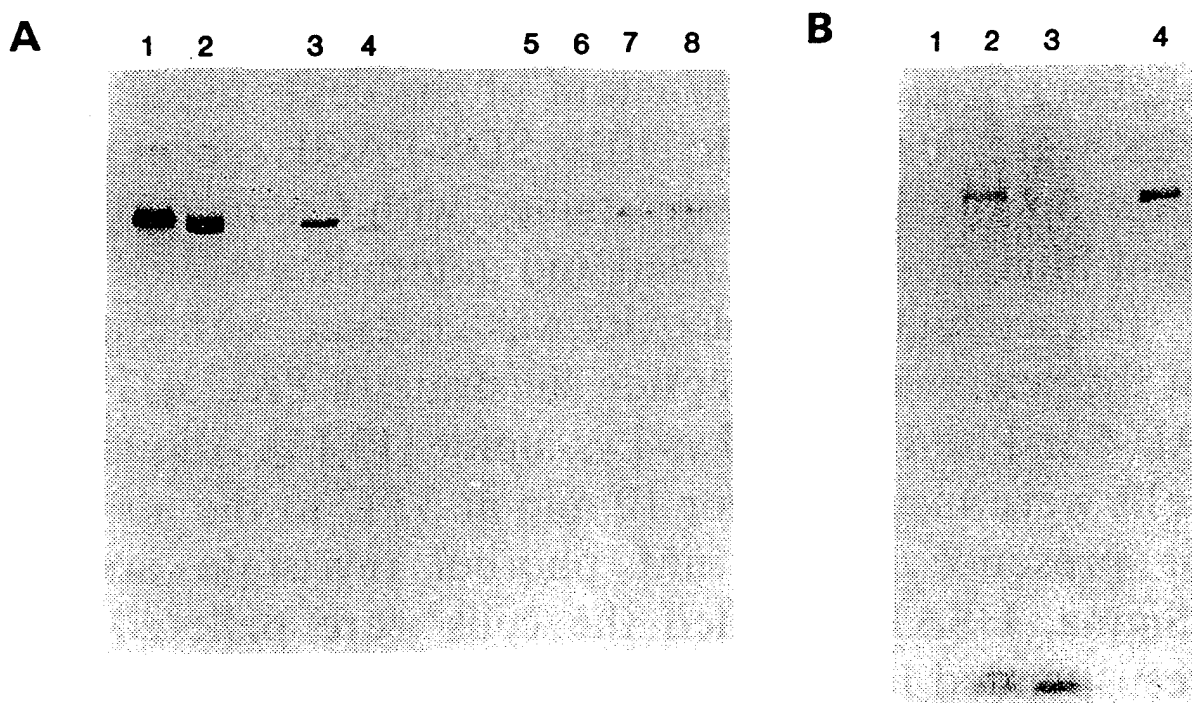
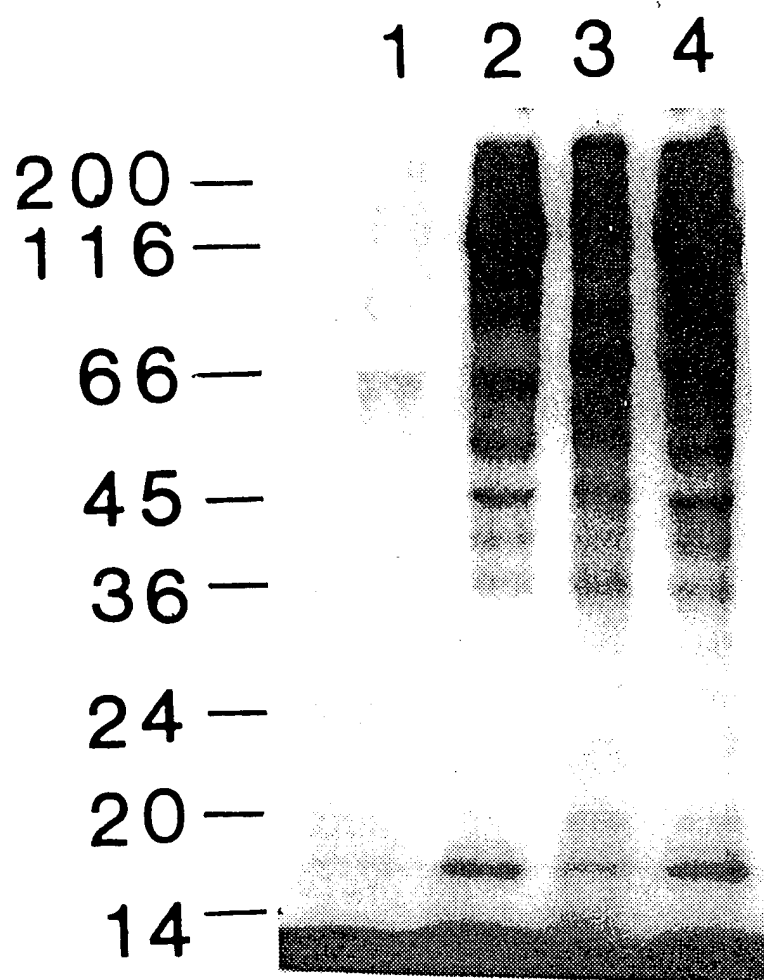


Figure 2. Phosphorylation of proteins in permeabilized lymphocytes and the effect of phorbol myristyl acetate. The phosphoprotein patterns are demonstrated by autoradiography of the ^{32}P -labeled protein bands obtained by SDS-PAGE. Lane 1: control cells, lane 2: control cells treated with phorbol myristyl acetate (40 ng/ml) in the course of permeabilization, lane 3: cells stimulated by phytohemagglutinin for 60 h, lane 4: cells stimulated by phytohemagglutinin for 60 h and treated with phorbol myristyl acetate (40 ng/ml) in the course of permeabilization.

Fig. 2



myristyl acetate on the phosphorylation of several other proteins, even in mitogen-stimulated cells was readily detectable (Fig. 2). Activation of protein kinase C by phorbol myristyl acetate was also tested by the incorporation of ^{32}P into the specific oligopeptide substrate of protein kinase C (13,14) and phorbol myristyl acetate caused about 700% and 420% increase in the phosphotransferase activity in resting and mitogen-stimulated cells, respectively (Table I).

The possible role of enzymes besides protein kinase C in the intracellular phosphorylation of poly(ADP-ribose) polymerase was also considered. poly(ADP-ribose) polymerase has already been reported not to be a substrate for protein kinase A (1). On the other hand the amino acid sequence (18) in the DNA-binding domain of this nuclear enzyme contains a region (Thr-Pro-Lys) that could be a target for the cyclin-dependent protein kinase 1-cdc2. The cell population stimulated by phytohemagglutinin for 60 h contained a significant number of cells in G2 phase, where cdc2 kinase is known to be active (19). For these reasons we tested *in vitro* the activity of cdc2 kinase with poly(ADP-ribose) polymerase as a substrate. While the cdc2 kinase phosphorylated H1 histone intensively, it was unable to catalyze the phosphorylation of poly(ADP-ribose) polymerase (Fig. 3A,B). Its role was also excluded when we found that poly(ADP-ribose) polymerase was phosphorylated in a cell population treated for only 16 h with phytohemagglutinin (Fig. 1B) which contained only a small percentage of cells in the G2 phase (Table II).

Table 1
 Activation of protein kinase C by phorbol myristate acetate in streptolysin-O- permeabilized cells with the specific oligopeptide as phosphate acceptor

Cells	Treatment with PMA	Phosphotransferase activity (cpm)
Resting	-	26 000
Resting	+	183 100
Stimulated	-	33 130
Stimulated	+	140 860

Cells were stimulated by phytohemagglutinin for 60 h and resting cells were maintained at suboptimal stimulation. Samples of stimulated and resting cells were incubated in the absence and presence of 100 nM PMA for 10 min at 37°C, then were pelleted and resuspended in the medium used for permeabilization (10^6 cells in 100 μ l medium). The activity of PKC was measured in the course of permeabilization. The phosphotransferase activity is expressed as the radioactivity of [32 P]phosphate incorporated into the selective oligopeptide substrate of PKC. The specific radioactivity of [γ - 32 P]ATP was $2.8 \cdot 10^5$ cpm/nmol.

Figure 3. Phosphorylation of purified poly(ADP-ribose) polymerase protein by a contaminating protein kinase and the ineffectivity of protein kinase 1-cdc2. Figures A and B show the results of attempts to phosphorylate poly(ADP-ribose) polymerase by the cyclin dependent kinase 1-cdc2: sample of H1 histone phosphorylated by cdc2 kinase (lane 1); a sample of purified poly(ADP-ribose) polymerase protein incubated in the absence of exogenous kinase (lane 2); sample of poly(ADP-ribose) polymerase protein incubated in the presence of cdc2 kinase (lane 3); poly(ADP-ribose) polymerase protein phosphorylated by protein kinase C (lane 4). The amount of cdc2 kinase preparation was 50 ng and the radioactivity of [32 P]ATP was 3×10^5 cpm per reaction mixture in experiments of Figure A and 200 ng cdc2 kinase preparation and 12×10^5 cpm per reaction mixture were used for experiments of Figure B. Arrows indicate the position of the protein band of poly(ADP-ribose) polymerase. Figures C and D show the phosphorylation of poly(ADP-ribose) polymerase by the contaminating kinase in the absence of activators or inhibitors (Fig. C lanes 1,3 and Fig. D lane 1); in the presence of 0.1 mM Ca $^{2+}$, 25 μ g/ml phosphatidylserine and 250 ng/ml diacylglycerol (Fig. C Lane 1); in the presence of 1 μ M staurosporin (Fig. C lane 2); in the presence of 200 μ M H7 (Fig. C lane 4 and Fig. D lane 2); in the presence of the pseudosubstrate inhibitory peptide of protein kinase C (200 μ M and 1 mM in Fig. D lanes 3 and 4, respectively); in the presence of DNA (12.5 μ g per reaction mixture, lane 5).

99

Fig. 3

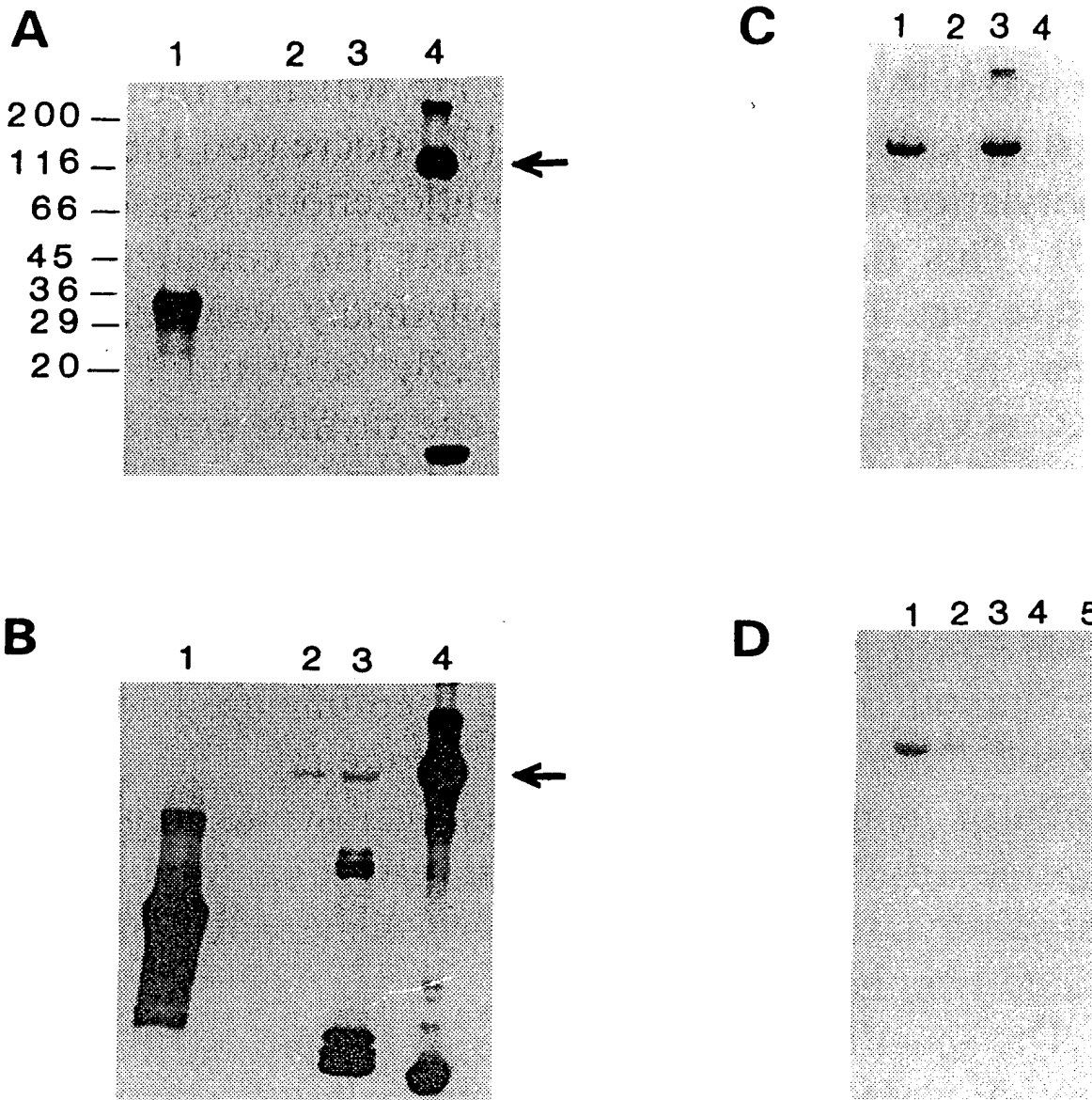


Table 2

Cell cycle distribution of lymphocytes and phosphorylation of PARP

Cells	G1 (%)	S (%)	G2 (%)	Phosphorylation of PARP
I. Resting	93	3	4	undetectable
II. Resting	95	2	3	undetectable
I. Stimulated for 60 h	65	23.5	11.5	detectable *
II. Stimulated for 16 h	87	8	5	detectable *

Cell cycle distribution and phosphorylation of PARP was determined as described under Materials and Methods.

* The specific radioactivity of these samples cannot be determined because of the unknown phosphorylation state by unlabeled ATP in cells.

However, in the course of experiments with cdc2 kinase we observed that our purified poly(ADP-ribose) polymerase preparations contained traces of a protein kinase activity, apparently as a contaminant, thus under appropriate circumstances poly(ADP-ribose) polymerase phosphorylation was detectable without the addition of protein kinase C (Fig. 3B,C,D).

The final step in the purification of poly(ADP-ribose) polymerase was affinity chromatography on m-benzamide agarose (15) and the poly(ADP-ribose) polymerase protein accounted for about 95% of isolated proteins. At this stage of purity a trace of protein kinase C phosphorylating poly(ADP-ribose) polymerase may be adsorbed to the enzyme because of the high affinity of protein kinases for their substrates. Therefore it is conceivable that this kinase catalyzes the intracellular phosphorylation of poly(ADP-ribose) polymerase. Although the contaminating kinase activity was not increased by the physiological activators of protein kinase C, it was inhibited by staurosporin and H7 (Fig. 3C) and by the pseudosubstrate inhibitory peptide which is a specific inhibitor of protein kinase C (20), and by DNA which inhibits the phosphorylation of poly(ADP-ribose) polymerase by protein kinase C (2) (Fig. 3D).

We also investigated the intracellular phosphorylation of poly(ADP-ribose) polymerase in the presence of inhibitors of protein kinase C. Under our experimental circumstances (i.e. the medium used for permeabilization contained both ^{32}P -labeled ATP and the inhibitor

compound) the pseudosubstrate peptide of protein kinase C was the most effective inhibitor of phosphorylation of poly(ADP-ribose) polymerase in phytohemagglutinin-stimulated lymphocytes (Fig. 4).

Figure 4. The effect of the pseudosubstrate inhibitory peptide of protein kinase C on the phosphorylation of poly(ADP-ribose) polymerase protein in phytohemagglutinin-stimulated lymphocytes. Phosphorylated poly(ADP-ribose) polymerase protein was immunoprecipitated, subjected to SDS-PAGE and the ^{32}P -labeling was demonstrated by autoradiography of the protein bands. Purified poly(ADP-ribose) polymerase protein phosphorylated by protein kinase C in vitro (lane 1), poly(ADP-ribose) polymerase ^{32}P -labeled in permeabilized lymphocytes (lanes 2-5): without inhibitor (lane 2), in the presence of 200 μM H7 (lane 3), in the presence of 1 μM staurosporin (lane 4) and in the presence of 1 mM protein kinase C pseudosubstrate inhibitory peptide (lane 5). Cells were treated with phytohemagglutinin for 40 h.

104

Fig. 5

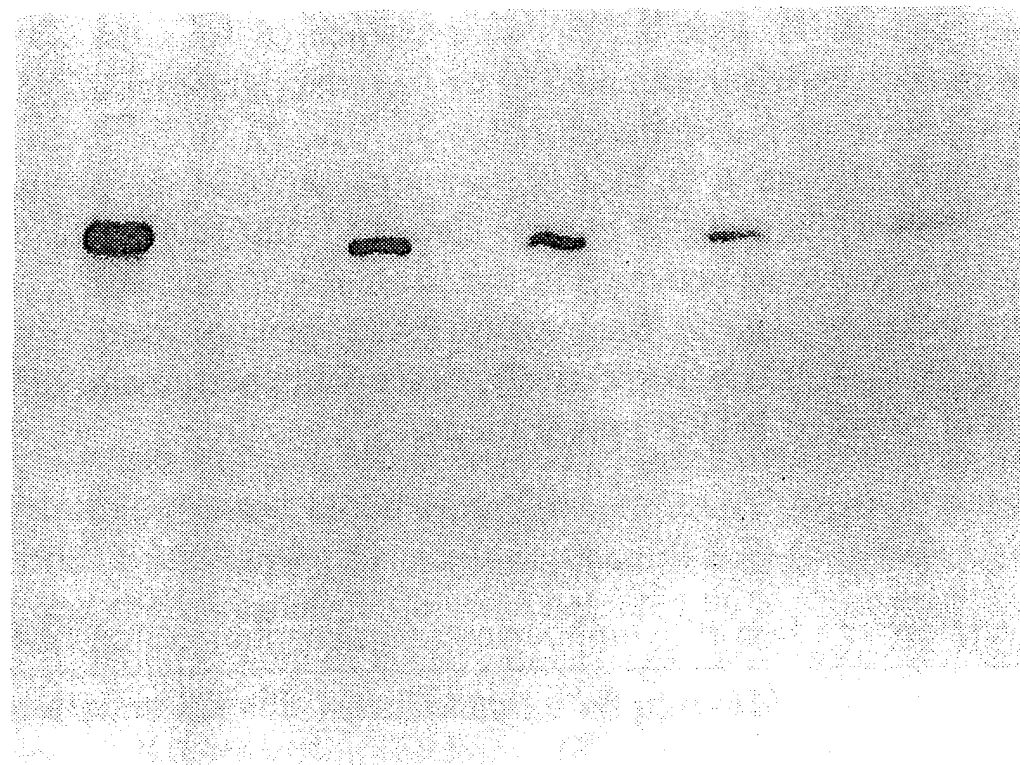
1

2

3

4

5



Discussion

Evidence presented supports the mechanism that connects protein kinase C activity with the regulation of poly(ADP-ribose) polymerase in a cellular system, albeit during cellular stimulation by a nonphysiological stimulant, phytohemagglutinin. This model may be eventually useful for the study of physiological cell stimulants (e.g. lymphokines). However the poly(ADP-ribose) polymerase inactivating effect of phytohemagglutinin-induced phosphorylation may explain the increased cellular toxicity of retroviral zinc finger oriented antiviral drugs in the presence of phytohemagglutinin (5) since both drugs and phytohemagglutinin depress cellular poly(ADP-ribose) polymerase activity by differing molecular mechanisms.

The mode of protein kinase C-catalyzed phosphorylation of poly(ADP-ribose) polymerase appears complex and require further comments. Since the effect of the pseudosubstrate peptide is accepted as a specific inhibition of protein kinase C activity in lymphocytes (10) we believe that in spite of the absence of stimulation by phorbol myristyl acetate the intracellular phosphorylation of poly(ADP-ribose) polymerase is probably catalyzed by a member of the protein kinase C family. Atypical subtypes of protein kinase C are not activated by phorbol myristyl acetate, therefore an atypical subtype may be responsible for the observed phosphorylation (21).

On the other hand, the possible role of a "classical" member (21) of the protein kinase C family is also conceivable. The endogenous protein kinase phosphorylating poly(ADP-ribose) polymerase that was found in the purified preparation of poly(ADP-ribose) polymerase protein may be identical with a proteolytically activated form of a classical protein kinase C isoenzyme (13,22). The failure of phorbol myristyl acetate to increase the intracellular phosphate incorporation into the poly(ADP-ribose) polymerase protein can be explained as well. One of the possible interpretations of this observation is that the poly(ADP-ribose) polymerase protein may not be available for protein kinase C in resting cells but becomes available in phytohemagglutinin-stimulated cells even in the absence of phorbol myristyl acetate. Although protein kinase C may be associated with the nucleus (23) the phosphorylation of poly(ADP-ribose) polymerase could occur in the cytoplasm. In resting cells the major part of poly(ADP-ribose) polymerase is localized in the nucleus and we have shown that the binding of poly(ADP-ribose) polymerase to DNA prevents the phosphorylation of the enzyme by protein kinase C (2). Phytohemagglutinin has been reported to increase the level of mRNA for poly(ADP-ribose) polymerase (6), thus it promotes the *de novo* synthesis of the enzyme protein mainly in the S phase (7). In phytohemagglutinin-treated cells a fraction of protein kinase C may become activated and the newly synthesized poly(ADP-ribose) polymerase protein could be a target of protein kinase C activity. Phosphorylation by protein kinase C inhibits the binding of poly(ADP-ribose) polymerase to DNA (2), and thus, with the aid of a phosphatase

(24), may regulate the binding of newly synthesized poly(ADP-ribose) polymerase to nascent DNA in the appropriate phase of the cell cycle.

References

1. Yoshihara, K., Tanaka, Y., Itaya,A., Kamiya, T. and Koide, S.S. (1987) Biochem. Biophys. Res. Commun. **148**, 709-711.
2. Bauer, P.I., Farkas, G., Buday, L., Mikala, G., Mészáros, G., Kun, E. and Faragó, A. (1992) Biochem. Biophys. Res. Commun. **187**, 730-736.
3. Kun, E. (1987) Adv. Exper. Med. Biol. **231**, 613-626.
4. Rice, W.R., Schaeffer, C.A., Harten, B., Villinger, F., South, T.L., Summers, M.F., Henderson, L.E., Bess, Jr., J.W., Arthur, L.O., McDougal, J.S., Orloff, S.L., Mendeleyev, J. & Kun, E. (1993) Nature **361**, 473-475.
5. Rice, W.G., Schaeffer, C.A.; Graham, L., Ming-Bu; McDougal, J.S., Orloff, S.L.; Villinger, F., Young, M., Oroszlan, S., Fesen, M.R., Pommier, Y., Mendeleyev, J. and Kun, E. (1993) Proc. Natl. Acad. Sci. USA **90**, 9721-9724.
6. Menegazzi, M., Carcereri de Prati, A., Miwa, M., Suzuki, H. and Libonati, M. (1992) Biochem. Internat. **26**, 69-77.
7. Wein, K.M., Netzker, R. and Brand, K. (1993) Biochem Biophys. Acta **1176**, 69-76.
8. Boyum, A. (1968) Scand. J. Clin. Lab. Invest. **21** (suppl. 97), 31-50.
9. Nicoletti, I., Migliorati, G., Pagaliacci, Grignani, F. and Riccardi, C. (1991) J. Immunol. Methd. **139**, 271-279.

- 10 Alexander, D.R., Hexham, J.M., Lucas, S.C., Graves, J.D., Cantrell, D.A. and Crumpton, M.J. (1989) Biochem. J. **260**, 893-901.
11. Sambrook, J., Fritsch, E.F. and Maniatis, T. (1989) Molecular Cloning. A laboratory Manual (2nd ed.) CHS Lab. Press, pp. 18.30-18.46.
12. Buki, K.G., Kirsten, E. and Kun, E. (1987) Anal. Biochem. **167**, 160-167.
13. Romhányi, T, Seprodi, J., Antoni, F., Mészáros, G., Buday, L. and Faragó, A. (1986) Biochim. Biophys. Acta **888**, 325-331.
14. Buday, L., Seprodi, J., Farkas, G., Mészáros, G., Romhányi, T., Bánhegyi, G., Mandl, J., Antoni, F. and Faragó, A. (1987) FEBS Lett. **223**, 15-19.
15. Bauer, P.I., Buki, K.G. and Kun, E. (1990) FEBS Lett. **273**, 6-10.
16. Buday, L. and Faragó, A. (1990) FEBS Lett. **276**, 223-226.
17. Berry, N. and Nishizuka, Y. (1990) Eur. J. Biochem. **189**, 205-214.
18. Kurosaki,T., Ushiro, H., Mitsuchi, Y., Suzuki, S., Matsuda, M., Matsuda, Y., Katunuma, N., Kangawa, K., Matsuo, H., Hirose, T., Inayama,S. and Sizuta,Y. (1987) J. Biol. Chem. **262**, 15990-15997.
19. Norbury, C. and Nurse, P. (1992) Ann. Rev. Biochem. **61**, 441-470.
20. House, C. and Kemp, B.E. (1987) Science **238**, 1726-1728.

21. Nishizuka, Y. (1992) Trends in Biochem. Sci. **17**, 414-417.
22. FaragóA. and Nishizuka, Y. (1990) FEBS Lett. **268**, 350-354.
23. Hug, H. and Sarre, T.F. (1993) Biochem. J. **291**, 329-343.
24. Bakó, E., Dombrádi, V., Erdödi, F. Zumo, L., Kertai, P. and Gergely, P. (1989) Biochim. Biophys. Acta **1013**, 300-305.

**SPECIFIC DISULFIDE FORMATION IN THE
OXIDATION OF HIV-1 ZINC FINGER PROTEIN
NUCLEOCAPSID P7**

Summary

In vitro oxidation of the HIV-1 nucleocapsid protein p7 by the C-nitrosocompound 3-nitrosobezamide (NOBA) has been investigated. When reconstituted p7 was incubated with NOBA, three disulfide bonds were formed per molecule of p7, Cys 15 - Cys 18, Cys 28 - Cys 36 and Cys 39 - Cys 49. These were identified using the proteolytic enzyme endoproteinase Lys-C and mass spectrometry. When the denatured protein (apo-p7) was incubated with NOBA, a more random pattern of multiple S-S linkage was found. Oxidation of reconstituted p7 also occurred on treatment with cupric ion and the same three major disulfide bonds were formed as in the reaction with NOBA. These results suggests the interpretation that the oxidation reaction occurs at the zinc-binding centers while zinc cations are still bound and that the two zinc fingers are not identical in their chemical properties. This latter point is consistent with the independent biological roles reported previously for the two fingers in the viral infection cycle.

Introduction

The retroviral nucleocapsid protein of human immunodeficiency virus HIV-1 contains two CCHC type zinc fingers (1-3), each of which binds zinc stoichiometrically with three cysteine thiols and a histidine imidazole group (4-6). These zinc complexes and the protein folding that they stabilize are essential for viral genome recognition during budding, genomic RNA packaging, and early events in viral infection (7-9).

Nuclear magnetic resonance experiments (10) have demonstrated that an 18-residue peptide with HIV-1 nucleocapsid N-terminal zinc finger sequence ejected zinc when it was treated with C-nitroso compounds. The same peptide had been shown previously to have sequence-dependent, high-affinity binding to oligonucleotide d(ACGCC) (11). Addition of 3-nitrosobenzamide (NOBA) and 6-nitroso-1,2-benzopyrone resulted in the dissociation of the complex, indicating the loss of the "finger" domain.

This susceptibility of retroviral zinc fingers is currently being exploited in the design of new agents with potential antiviral activity. Mutation of either of the two zinc fingers in the native HIV-1 nucleocapsid protein p7 yields noninfectious virus (7,9), which suggests that the zinc fingers are ideal targets for the development of new antiviral drugs. The antiviral activity of NOBA has been demonstrated against HIV (12) and against SIV (13) in cell culture.

A detailed characterization of the reaction between the complete viral zinc finger protein p7 and C-nitroso compounds is of interest to search for more effective antiviral drugs. In this report, we identify the products found in vitro in the reaction between the p7 protein and NOBA as a representative C-nitroso oxidizing agent. Only three disulfide bonds were identified by proteolytic cleavage and mass spectrometric analysis. This same specificity was also observed in the oxidation of p7 by cupric ion. The pattern of disulfide formation are different in the two zinc complexes, consistent with an earlier observation (9) that the two zinc fingers in the p7 are not functionally equivalent. A more diverse set of disulfide bonds was formed in control reactions using demetallated apo p7.

Experimental Section

Chemicals. 3-Nitrosobenzamide (NOBA), m.p. 135 °C (decomp), was prepared by the oxidation of 3-aminobenzamide (Aldrich, Milwaukee, WI) by 2 equivalent of 3-chloroperoxybenzoic acid in dimethyl formamide solution at 5 °C as described previously (14). High-resolution EIMS: calcd for C₇H₆N₂O₂ 150.0429; found M⁺ (M/Z): 150.0429 3,3'-Dicarbamoylazoxybenzene (the dimeric azoxy derivative of NOBA), m.p. 280-284 °C (decomp), was isolated as a side product (precipitate) from the NOBA synthesis reaction. High-resolution EIMS: calcd for C₁₄H₁₂N₄O₃ 284.0909; found M⁺ (M/Z): 284.0903.

Protein preparation. The coding sequence for the nucleocapsid protein of HIV (p7) was cloned and expressed in *Escherichia coli* using an inducible expression vector p-Mal (New England Biolabs, MA). The protein was released from a fusion protein by proteolysis with Factor Xa, and purified as apo-p7 by reversed phase high performance liquid chromatography (HPLC). The protein was characterized by both microchemical and mass spectrophotometric amino acid sequencing (2,15).

The p7 protein was reconstituted at 15 μM concentration in 50 mM Tris/HCl buffer at pH 7.5 with two equivalent of ZnCl₂ to generate native protein and its folded structure. The reconstituted Zn₂-p7 protein

complex was also characterized as a three partner noncovalent complex by electrospray ionization mass spectrophotometry (15,16).

Oxidation of reconstituted p7. The reconstituted p7 protein was treated with 20 molar equivalents of NOBA or 10-fold excess of cupric chloride in 50 mM Tris-HCl buffer at pH 7.5. The reaction products of p7 were purified from reversed phase HPLC using a C8 column (Aquapore RP-300, 4.6 x 250 mm, Applied Biosystems, San Jose, CA), and a solvent gradient :).08% trifluoroacetic acid in acetonitril 10% to 40% in 20 min., in 0.1% trifluoroacetic acid in water.

Oxidation of denatured apo p7. HIV-1 nucleocapsid protein p7 was denatured and separated from zinc cations on reversed phase HPLC at pH 2. The apoprotein was collected and freeze-dried. Reaction between 1 ml of a 15 μ M solution of the apoprotein and 20 molar equivalents of NOBA were carried out at pH 7.5 (50 mM Tris-HCl)at 37 °C, for times varied between 5 and 120 minutes and were monitored by HPLC.

Mass spectrometric analysis. Electrospray ionization mass spectrometry (ESMS) was performed on a Vestec (Houston, TX) electrospray source fitted to a Hewlett-Packared (Palo Alto, CA) 5988A quadrupole mass spectrometer. All ions were detected with Phrasor (Duarte, CA) high energy dynode ion detector, and data was collected with a Technivent (St. Louis, MO) Vector II software system. Samples

were injected through a Rheodyne (Cotati, CA) 7125 loop injector fitted to a Harvard syringe pump (South Natick, MA) at 10 μ l/min. flowrate. The stainless steel needle was held around 2.2 kV and the source temperature was maintained at 240 °C. All samples were first dissolved in 6% acetic acid and then mixed with an equal volume of methanol. The instrument was calibrated using melittin and myoglobin.

Matrix assisted laser desorption mass spectrometry was carried out on a Kratos/Shimadzu Kompact III instrument, using the reflectron mode with a 337 nm UV laser. The matrix was α -cyano-4-hydroxycinnapinic acid used in a ratio to the sample of about 10000:1. Prepro nerve growth factor and the protonated matrix dimer were used as external mass calibrants.

Fast atom bombardment (FAB) mass spectrometry was performed on the first two sectors of a JEOL HX110/HX110 tandem mass spectrometer (Tokyo, Japan). A JEOL FAB gun was operated at 6 kV with xenon as FAB gas. The accelerating voltage was 10 kV. Thioglycerol was used as the FAB matrix. The resolution was set at 500, and all data was collected with a JEOL DA 7000 data system. All molecular weights reported here are averages (17).

Proteolysis of oxidized p7 and apo p7. Oxidized proteins (80 μ g) were hydrolyzed by endoproteinase Lys-C (Boehringer Mannheim, Manheim, Germany) without dithiothreitol, in 100 mM potassium

phosphate at pH 7.9. The proteolysis was carried out at 37 °C for 10-15 min. with a protease/protein ratio (w/w) of 1:50.

Peptide mixtures were purified on reverse phase HPLC (Aquapore RP 300 column, 4.6 x 250 mm, Applied Biosystems). The solvent gradient was 0.08% trifluoroacetic acid in acetinitril (5% to 45% in 40 min.) in 0.1% trifluoroacetic acid in water. Resolved peptides from reconstituted p7 were analyzed by electrospray and fast atom bombardment mass spectrometry. Peptides from apo p7 were analyzed by laser desorption mass spectrometry.

RESULTS

Reaction of NOBA and Cu²⁺ with Zn-reconstructed p7. A solution of p7 reconstituted with zinc was incubated with NOBA as described in the experimental section. The reaction was followed by reverse phase HPLC. The peak comprising apo p7 decreased in size and an asymmetric peak appeared at shorter retention time (Figure 1). (Under chromatographic conditions at pH 2, zinc is lost and the protein elutes as apo-p7). The product was collected as one fraction from HPLC and characterized by ESMS (Figure 2). The major component was found to have a molecular weight of 6445.3 daltons. Apo p7 has a calculated molecular weight of 6451.7 daltons, determined by ESMS as 6451.3 daltons. Thus the major product from the reaction of NOBA weighs 6 daltons less than apo-p7. The new protein was reduced by 2-mercaptoethanol to a protein that coeluted with apo-p7, consistent with disulfide formation.

Cupric chloride was also incubated with Zn-reconstructed p7. The chromatogram was similar to that from the NOBA reaction, and the peak are of apo-p7 was reduced by about half after 6 minutes. ESMS showed that the modified protein mixture has a molecular weight of 6445.7 daltons, again 6 daltons less than that of apo-p7. Two minor peaks eluting

Figure 1. Analysis of p7 reactions with NOBA by reversed phase high performance liquid chromatography. a./ NOBA reagent before reaction with p7 (The sharp peak near the end of elution corresponds to the dimeric azoxy derivative of NOBA); b./ p7 protein before reaction; c./ p7 and NOBA reaction mixture after 2 hours of incubation; d./ apo-p7 and NOBA after two hours of incubation

Fig. 1

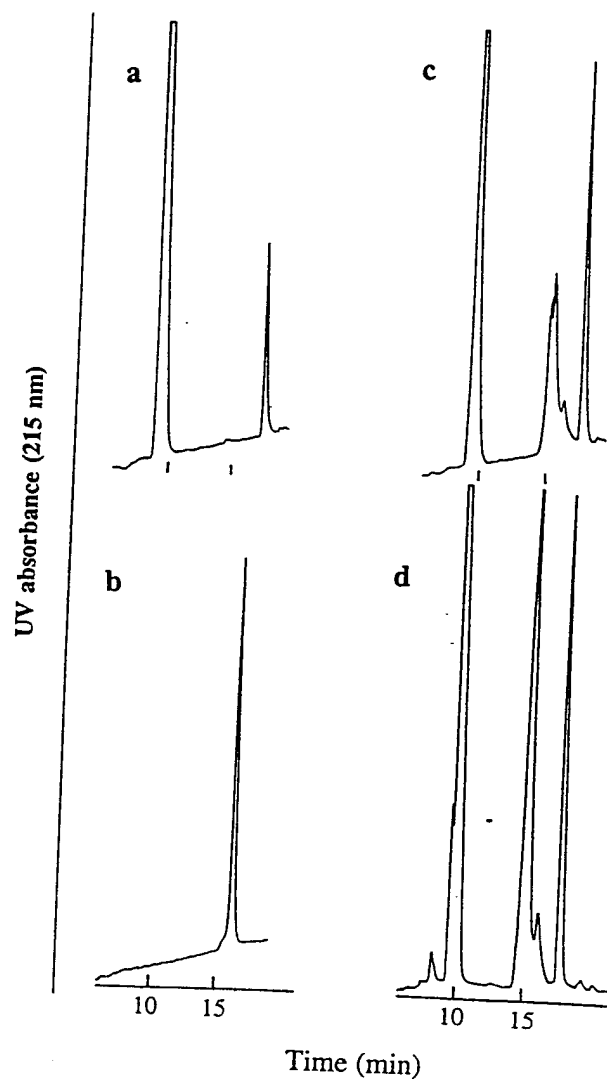
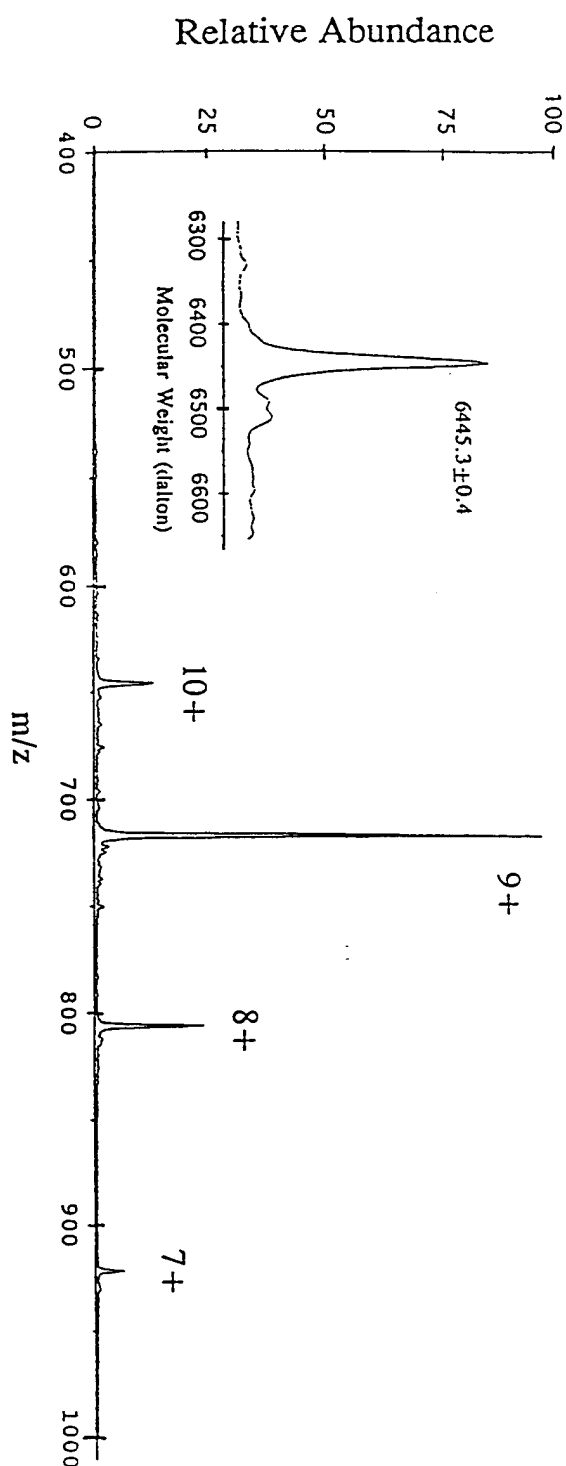


Figure 2. Mass spectrum of the peak eluting at 15 min produced by the reaction of NOBA with p7 (Figure 1c)

Fig. 2



after the apo-p7 peak were found to have molecular weights of 12896.6 dalton. These were not examined further in this study.

Reaction of NOBA with apo-p7. The products formed in this control reaction eluted in a new peak with shorter retention time under the same HPLC conditions used for the previous two analyses. This material was also found to have molecular weight of fully oxidized p7 (6445.2 daltons).

Identification of the positions of disulfide bonds. Oxidized proteins purified from NOBA-p7, Cu²⁺-p7 and NOBA-apo p7 reactions were subjected to endoproteinase Lys-C hydrolysis. The molecular masses of the resulting peptides were determined by both ESMS and FABMS. Disulfide bridges were identified by comparing the observed masses of the fragments to the theoretical masses of peptides resulting from all possible disulfide pairings. Peptides were also mapped from reduced apo p7 as a control.

For the NOBA-p7 and Cu²⁺-p7 reactions, fragments without Cys were easily identified on the basis of their measured and calculated molecular masses (Table 1). three major peaks with molecular masses of 668.8, 1472.8 and 1933.0 daltons ere also detected, which uniquely matched and were assigned as peptides [15-20], (Cys15-Cys18); [27-38], (Cys 28- Cys 36); and [39-55], (Cys 38 - Cys 49). As further confirmation the peptides were converted to their methyl esters and appropriate molecular masses

Table 1. Molecular Masses of peptides produced by endoproteinase Lys-C from NOBA- and Cu²⁺-oxidized p7^a

peptide	calculated MW ^b (apo-p7)	observed MW (apo-p7)	observed MW (NOBA)	observed MW (Cu ²⁺)
[1-11]	1434.6	1435.1	1434.0	1434.0
[12-14]	372.5	372.5	372.8	372.7
[15-20]	670.8	670.6	668.8	669.2
[21-26]	653.7	653.6	653.7	653.0
[27-38]	1474.8	1474.2	1472.8	1472.6
[39-55]	1935.2	1935.2	1933.0	1932.9

- a. Sequence of p7 protein:
 MQRGNFRNQRKIIKC¹⁵FNC¹⁸GKEGHIAKNC²⁸RAPRKRGCC³⁶WKC³⁹GKEGHQMKDC⁴⁹TERQAN
- b. Molecular weights are calculated for unmodified peptides from reduced apo-p7 as isotopic averages (17).

were determined (data not shown). As shown in Table 1 the complete sequence of 55 residues were accounted for.

The same proteolytic cleavages and disulfide linkages were identified in p7 oxidized by Cu²⁺ ions (Table 1). Three disulfide containing peptides were identified with molecular masses of 669.2, 1472.5 and 1932.9 daltons. These are consistent with pairing between the two cysteines within each peptide, [15-20], [27 -38], and [39 - 55], respectively.

To elucidate the determinants of this specific pattern of S-S pairing, apo p7 was incubated with NOBA. Digestion of the reaction product with endoproteinase Lys C resulted in a larger mixture of peptides (Table 2). All possible disulfide pairs were detected, except the linkage between Cys-36 and Cys-49. This wide variety stands in contrast to the trio formed in the folded protein. Table 3 summarizes the different patterns.

Table 2 Molecular masses of peptides produced by endoproteinase Lys-C from NOBA-oxidized Apo-p7

observed MW	peptide	Calculated MW ^a
669.1	[15-20]	668.8
935.3	[34-41]	935.2
1148.6	[27-33] + [39-41]	1148.4
1241.1	[39-41] + [48-55]	1240.3
1491.8	[27-33] + [34-38]	1490.8
1778.3	[27-33] + [48-55]	1778.0
1318.0	[15-20] + [34-38]	1317.6
1513.5	[15-20] + [27-33]	1512.8
1622.4	[15-20] + [34-38] + [39-41]	1622.0
2159.3	[15-20] + [27-33] + [34-38]	2159.6
2251.3	[15-20] + [34-38] + [48-55]	2251.5

^aMolecular weights are calculated for oxidized peptides from apo-p7 as isotopic averages (17).

Table 3. Disulfide bonds detected after NOBA treatment

Disulfide bonds	reconstituted p7	apo-p7
Cys15-Cys18	+	+
Cys15-Cys28, Cys18-Cys36*	-	+
Cys15-Cys28, Cys18-Cys39*	-	-
Cys15-Cys28, Cys18-Cys49*	-	-
Cys15-Cys36, Cys18-Cys39*	-	+
Cys15-Cys36, Cys18-Cys49*	-	+
Cys15-Cys39, Cys18-Cys49*	-	-
Cys28-Cys36	+	+
Cys28-Cys39	-	+
Cys28-Cys49	-	+
Cys36-Cys39	-	+
Cys36-Cys49	-	+
Cys39-Cys49	+	+

a. or alternative isomeric linkages

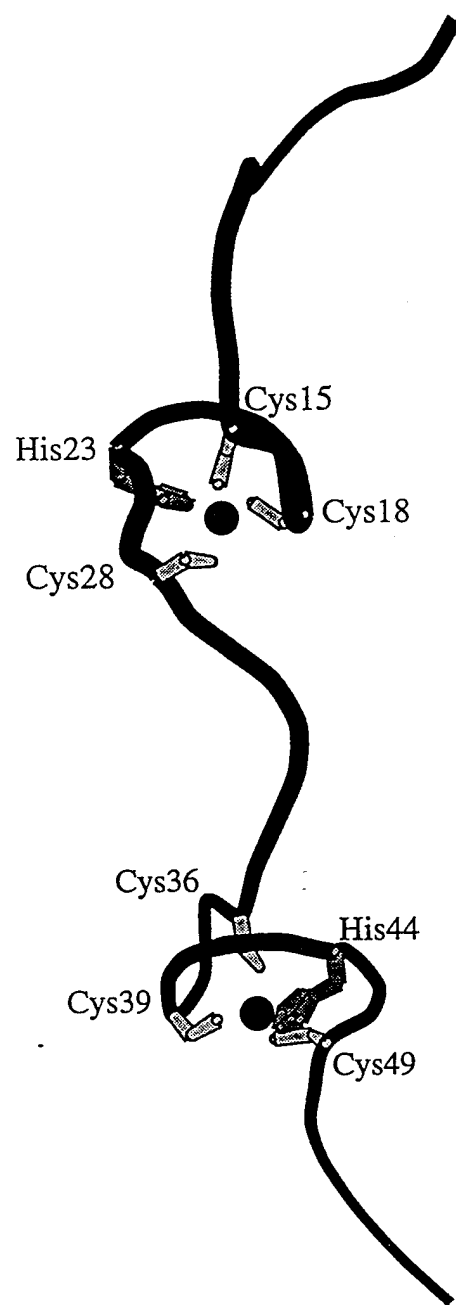
Discussion

It was demonstrated previously that zinc was ejected and the three dimensional folding was lost when a synthetic HIV-1 zinc finger peptide was treated with NOBA and NOBP (10). However, the reaction products were not determined. An oxidative mechanism of action of NOBP on poly(ADP-ribose) polymerase, which also contains two retroviral CCHC-type zinc fingers, has been proposed (18, 19). Furthermore, the two zinc fingers in the HIV-1 nucleocapsid protein p7 were found not functionally equivalent, suggesting an independent role of each finger in viral RNA selection and packaging (9). The susceptibility of the two zinc fingers in the native p7 protein towards oxidizing reagents and their importance in the viral infectious cycle justifies the determination of chemical mechanisms.

Since there are three cysteines in each zinc finger (Figure 3) and a total of six cysteines in HIV-1 nucleocapsid protein p7, a molecular weight decrease of six daltons in p7 after the NOBA treatment suggests the formation of three disulfide bonds. Such an oxidation reaction is predictable because C-nitroso compounds are known to be oxidizing agents towards thiols (18, 19). In other experiments we have determined that NOBA is reduced to 3-hydroxylaminobenzamide by way of p7 adducts. Molecular weights of p7 adducts were observed by ESMS at 6602.4 and 6751.9 daltons consistent with covalent bond formation.

Figure 3. Backbone representation of HIV-1 NC protein adapted from Summers et al. (1992) reference #21.

The structure presented was transformed from ribbon model using molscript program. Balls represent the two zinc atoms; the amino acid residues chelating the zinc atom are pointed out from the main chain.



between cysteine sulfur and nitroso nitrogen atoms of 1 an 2 NOBA molecules. The hydroxylamino species at neutral pH readily dismutates and condenses with unreacted nitroso molecules to form the stable dimeric azoxy derivative 3,3'-dicarbamoylazoxylbenzene, a process that commonly occurs during the mild reduction of aromatic nitroso compounds (30).

The more promiscuous pattern of disulfide pairing found to occur in the demetalled and denatured protein suggests that oxidation of the native or reconstituted protein by NOBA occurs at the Zn-binding centers while metal cations are still bound.

Closer examination of the oxidation of reconstituted p7 reveals differences in the disulfide linkages formed within each of the two zinc fingers, Cys 15 - Cys 18 in finger 1 and Cys 39 - Cys 49 in finger 2. In one case the disulfide bond is connected with two intervening amino acid residues and in the other case with nine. It seems likely that the geometry and distribution of electron densities within the metal chelate coordinates disulfide pairing in a specific manner.

Asymmetry in the CCHC-type metal complexes may promote uneven electron distributions among the three thiolate centers in each finger (Figure 3). In addition three different types of NH-S hydrogen bonds are present within each zinc finger, and there is a unique hydrogen bonding between a glutamine side chain and cysteine sulfur in the N-terminal

finger (21, 22). Combined with the specific sequences within the each of the zinc binding motifs, these properties may result in different reactivities of the various cysteine residues towards NOBA. Differences in the chemical reactivities of the two zinc fingers in the HIV-1 nucleocapsid protein are consistent with earlier observations (9) of functional differences and the independent role of each finger in viral RNA selection and packaging and viral infection.

It is interesting that Cu^{2+} produced the same intramolecular disulfide pattern in the oxidation of p7. Since the oxidizing reagents are quite different, this further suggests that the intramolecular oxidation reaction is largely dependent on the chemical properties of metal-binding cysteines.

References

1. Berg, J.M. (1986) *Science* **232**, 485-487.
2. Henderson, L.E., Bowers, M.A., Sowder II, R.C., Seebyn, S.A., Jihnon, D.G., Bess Jr, J.W., Arthur, L.O., Bryant, D.K., And Fenselau, C. (1992) *J. Virol.* **66**, 1856-1865.
3. Bess Jr, J.W., Powell, P.J., Issaq, H.J., Schumack, L.J., Grimes, M.K., Henderson, L.E. and Arthur, L.O. (1992) *J. Virol.* **66**, 840-847.
4. South, T.L. and Summers, M.F. (1990) in *Advances in inorgainc biochemistry* (Marzilli, L.G. and Eichhorn, G. Eds.) pp 191-248, Elsevier Science Publishing, Inc., New York.
5. South, T.L., Kim, B., Hare, D.R. and Summers, M.F. (1990) *Biochem. Pharmacol.* **40**, 123-129.
6. Chance, M.R., Sagi, I., Wirt, M.D., Frisbie, S.M., Scheuring, E., Bess Jr, J.W., Henderson, L.E., Arthur, L.O., South, T.L., Perez-Alvarado, G. and Summers, M.F. (1992) *Proc. Natl. Acad. Sci. USA* **89**, 10041-10045.
7. Aldovini, A. and Young, R.A. (1990) *J. Virol.* **64**, 1920-1926.

8. Gorelick, R.J., Nigida, S.M., Bess Jr, S.W., Arthur, L.O., Henderson, L.E. and Rein, A. (1990) *J. virol.* **64**, 3207-3211.
9. Gorelick, R.J., Chabot, D.J., Rein, A., Henderson, L.E. and Arthur, L.O. (1993) *J. Virol.* **67**, 4027-4036.
10. Rice, W.R., Schaeffer, C.A., Harten, B., Villinger, F., South, T.L., Summers, M.F., Henderson, L.E., Bess, Jr., J.W., Arthur, L.O., McDougal, J.S., Orloff, S.L., Mendeleyev, J. & Kun, E. (1993) *Nature* **361**, 473-475.
11. South, T.L. and Summers, M.F. (1993) *Protein Sci.* **2**, 3-19.
12. Rice, W.G., Schaeffer, C.A.; Graham, L., Ming-Bu; McDougal, J.S., Orloff, S.L.; Villinger, F., Young, M., Oroszlan, S., Fesen, M.R., Pommier, Y., Mendeleyev, J. and Kun, E. (1993) *Proc. Natl. Acad. Sci. USA* **90**, 9721-9724.
13. Chuang, A.J., Killam Jr., K.F., Chuang, R.Y., Rice, W.G., Schaeffer, C.A., Mendeleyev, J., Kun, E. (1993) Inhibition of the replication of native and 3'-azido-2',3'-dideoxythymidine (AZT)-resistant simian immunodeficiencyvirus (SIV) by 3-nitroso-benzamide. *FEBS Lett.* **326**, 140-144.
14. Kun, E., Mendeleyev, J. and Rice, W.G. (1993) U.S. Patent Ser. No. 08/087, 566 pending.

15. Fenselau, C., Yu, X., Bryant, D., Bowers, M.A., Sowder II, R.C. and Henderson L.E. (1994) in: In Mass spectrometry for the characterization of microorganisms (Fenselau, C., Ed.) pp 159-172, ACS Symposium Series 541, Washington, D.C.
16. Yu, X., Wojciechowski, M. and Fenselau, C. (1993) Anal. Chem. **65**, 1355-1359.
17. Yergey, J., Heller, D., Hansen, G., Cotter, R.J. and Fenselau, C. (1983) Anal. Chem. **55**, 353-356.
18. Buki, K.G., Bauer, P.I., Mendeleyev, J., Hakam, A., Kun, E. (1991) FEBS Lett. **290**, 181-185.
19. Buki, K.G., Bauer, P.I., Mendeleyev, J., Hakam, A. and Kun, E. (1992) in: ADP-ribosylation Reactions (Poirier G.G. and Moreau, P., Eds.) pp 329-333, Springer-Verlag, New York.
20. Coombes, R.G., (1979) in: Comprehensive Organic Chemistry (Southerland, I.O., Ed.) Chapter 7, p 317, Pergamon Press, Oxford.
21. Summers, M.F., Henderson, L.E., Chance, M.R., Bess Jr, J.W., South, T.L., Blake, P.R., Sagi, I., Perez-Alvarado, G., Sowder II, R.C., Hare, D.R. and Arthur, L.O. (1992) Protein Sci. **1**, 563-574.